Geometrical Mangrove Models

MSc Thesis

by

K.F. Jerez Nova

Cover Image: Grey Mangroves (Avicennia marina) in an estuary near Bonnie Vale in the Royal National Park, Australia

Geometrical Mangrove Models

Quantifying frontal surface area distribution for Avicennia marina vegetation: an important parameter for estimating wave attenuation

by

K.F. Jerez Nova

in partial fulfillment of the requirements for the degree of

Master of Science

in Civil Engineering

at the Delft University of Technology,
to be defended publicly on 22 September, 2022 at 10:45 AM

Student number:	4287940	
Project duration:	October 1, 2021 – September 22, 2022	
Thesis committee:	Dr. B.K. van Wesenbeeck,	TU Delft/Deltares, chair
	Dr. ir. B. Hofland,	TU Delft
	Ir. A.G.M. Gijón Mancheño,	TU Delft, supervisor
	Ir. S.A. Kalloe,	TU Delft

TU Delft

Preface

This thesis marks the end of my studies pursuing a Master's degree in hydraulic engineering. My interests in engineering and water-related societal problems made me follow this study track, and I have not regretted it for a second. It has been a great pleasure to work on this thesis. The combination of nature-based flood defences (mangroves) with a computational modelling approach is what fascinated me most. I truly believe that software applications can, in the future, improve hydrodynamic modelling where vegetation is involved. Hopefully, I will be able to transfer some of my enthusiasm about this topic and provide insightful tools for further research that may create more awareness of the importance of mangrove systems worldwide.

First, I would like to thank the committee members: Bregje van Wesenbeeck, Bas Hofland, Alejandra Gijón Mancheño and Su Kalloe. Thank you all for being so approachable and providing me with helpful feedback when needed. Your suggestions have significantly improved the quality of the report. The periodic meetings were always exciting and gave me new ideas. The measurement campaign in the greenhouse was a unique experience that I will always carry with me. I am grateful for the opportunity to conduct experiments and the trust you all gave me.

I also want to thank Grada, Darwin, Matthijs, Lisa and Lynn for their unconditional love and support during my studies.

K.F. Jerez Nova
Delft, September 2022

Summary

To estimate wave attenuation by mangrove forests, trees are often schematized as uniform cylinders (over the height) representing a tree's stem. However, trees have more complex geometrical features that influence the interaction between waves and tree structures. Recent studies have shown that the frontal surface area distribution over the height $Av(z)$ is a crucial parameter for estimating wave attenuation by vegetation (Kalloe et al., 2022; van Wesenbeeck et al., 2022) because it can account for complex geometrical features. This study aims to model the complex geometry of the *Avicennia marina* mangrove species. The research question then becomes:

How to construct geometrical tree models of Avicennia marina vegetation and how to obtain the projected frontal surface area distribution over the height, $Av(z)$?

Methodology

In this study, manual measurements were performed to obtain tree structure parameters. Both canopy and root measurements were conducted for *Avicennia marina* vegetation with varying characteristics (age and density). Two saplings (approximately 1.5 years old) with variable canopy densities and two young trees (around five years old) with varying canopy densities were measured. We stored canopy measurements in a so-called tree data structure consisting of nodes (representing the branches) that contain information about the individual branches, such as branch orders, -lengths and -diameters and edges, which are links that establish direct relations from one branch to another. After that, we developed a search tree algorithm to loop through all tree data, compute parameters of interest and store the results in assigned data arrays. Parameters of interest to obtain after the data analysis were branch dimensions and diameter ratios of branches (between various branch classes). This information was necessary to create a blueprint for constructing geometrical tree models.

Tree modelling started with the construction of a root (pneumatophore) model. Additionally, the frontal surface area of these roots was computed and displayed as a function of the height. In addition to the root model, we constructed two canopy models. The first model is based on relations between branches and can be called deterministic or dependent (canopy model 1). The second canopy model (canopy model 2) generates branch dimensions based on the normal distribution of branch diameters and is, therefore, more probabilistic with branches independent of each other.

Both canopy models construct branches based on information travelling from preceding branches. The models account for the proper placement of branches within 3D space by rotations and translations. The algorithm computes and outputs the projected frontal surface area over the height of a system of branches for a given direction (XZ-plane projection or YZ-plane projection). We validated the two canopy/tree models against validation measurements. Three trees were divided into seven vegetation layers, and branches were registered that intersected with the layers. As a result, estimation could be made on the frontal surface area per layer.

Results

This study found that the frontal surface areas due to roots and canopies are significant and are well represented by the parameter $Av(z)$. The contribution of the roots and canopy cannot be neglected in modelling wave dissipation by vegetation. The contribution of smaller branches to the total Av is significant, proving that considering only the tree stem is an underestimation. Moreover, the research shows that it is possible to develop a geometrical tree model based on a set of measurements and design rules that follow from observations, at least for the considered tree species. We could extrapolate and interpolate our results to generate tree models for a wide range of tree ages. Additionally, it is possible to create a forest by generating multiple trees.

Both tree models (1 and 2) showed little differences in $Av(z)$ during the model validation process. Moreover, the validation measurements led, in general, to an overestimation of the total frontal surface area. Consequently, model validation was inconclusive regarding both tree models. However, we found that constructing tree models according to tree/canopy model 1 is preferred because it resembles an L-system more and is more practically applicable in computer models.

We can improve future tree models by collecting more measurements regarding branch structures and root distribution as a function of tree age. This will result in increased model reliability.

Contents

1
Introduction

Mangroves are a group of tree species that inhabit the intertidal zone in (sub-)tropical coastal regions. The distribution of mangroves across the globe is shown in Figure 1.1 (Spalding et al., 2010). Mangroves thrive in brackish/salty and muddy environments with generally low incoming wave energy (McIvor et al., 2012). However, they may occasionally receive a substantial amount of wave energy, mainly when growing on the fringes of open bays and estuaries (Alongi, 2009). Mangroves provide vital ecosystem services such as increasing coastal resilience by attenuating waves (Mazda et al., 2006), trapping sediments to enhance soil formation and stabilizing the soil by its root systems (Yang et al., 2013; van Santen et al., 2007). These processes counteract coastal erosion and (relative) sea-level rise, which contributes to coastal stabilization (Lovelock et al., 2015). Additionally, mangrove canopies above the waterline considerably reduce the wind-induced shear stress on the water surface in case of non-submergence (Alongi, 2009). Mangrove forests are a prominent example of natural coastal protections just like other ecosystem-based flood defences such as salt marshes and seagrasses.

Figure 1.1: Global distribution of mangroves in yellow after Spalding et al. (2010)

Conventional, “hard” coastal defences such as dikes and seawalls often hinder the natural balance of sediments and water flow. Furthermore, they often require periodic heightening by rising sea levels. Ecosystem-based flood defences, such as mangrove forests, can be more sustainable and cost-effective as they can adapt to sea level rise (Temmerman et al., 2013). Unfortunately, a declining trend is visible in the total surface area of mangrove vegetation worldwide (Giri et al., 2011), with some mangrove species even at risk for extinction (Polidoro et al., 2010). Planting new mangrove forests often requires temporary protection at the foreshore, which allows trees to mature in calm conditions. The new forests need sufficient space, while urban and agricultural developments/coastal squeezing limits the area available for mangrove expansion or new mangrove areas. Consequently, it is easier to preserve and maintain already existing mangrove forests than to create new ones.

The importance of mangroves in terms of coastal protection is often neglected. This is partly due to the difficulty in accurately predicting the provided coastal protection potential. The promotion and conservation of mangrove trees for coastal management is currently hindered due to the uncertainty in their performance (Maza, Lara, et al., 2021). The complex geometry and highly dynamic environment in which mangroves exist makes it challenging to accurately predict wave- and current attenuation quantitatively.

Many factors determine the extent of wave energy dissipation by a mangrove forest, as illustrated in Figure 1.2. These include among others:

- Mangrove geometry: e.g., root structure, stem structure, canopy height and leave/branch density over the vertical height (Mazda et al., 2006). These geometrical characteristics partially depend on the type of mangrove species.
- Vegetation flexibility: reshaping of vegetation due to the loads exerted by waves and currents (Järvelä, 2004; Mazda et al., 2006).
- Mangrove zonation: forest length, -density and -age/growth level (Mazda and Wolanski, 2009; Maza, Lara, et al., 2021; McIvor et al., 2012).
- Hydraulic conditions: water depth, wave height and spectral characteristics (McIvor et al., 2012; Mazda et al., 2006).
- Foreshore characteristics (McIvor et al., 2012).

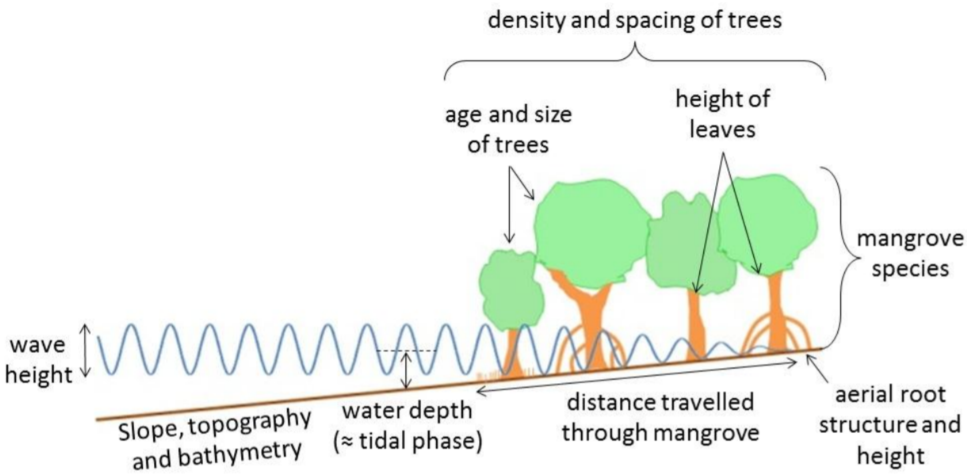

Figure 1.2: Governing factors for wave-vegetation interaction (McIvor et al., 2012).

The extensive list of factors affecting wave energy dissipation contributes to the complexity of investigating the effect of wave damping by mangrove vegetation in coastal areas. Because of this complexity, some factors such as the geometry of tree structures are being simplified. This simplification may potentially come at the expense of accurately predicting the wave attenuation behaviour, which brings us to the following problem statement.

1.1. Problem statement

Currently, hydrodynamic modelling for mangrove trees is too simplistic because mangrove trees are often schematized as rigid cylinders using information about the roots and trunk, thereby neglecting the canopy and complex root systems. Neglecting the canopy may be a reasonable assumption to model wave attenuation by relatively older specimens (where the canopy is located far above ground level), and/or for relatively low water levels. However, the canopy will be submerged for young vegetation and/or for older specimens during high water levels. Moreover, the canopy will experience wind loads during storms, and if we want to assess tree stability estimates are needed of the canopy area.

In reality, mangroves have complex geometry and exhibit differences in shape and orientation over the vertical coordinate. For example, the canopy often consists of leaves and branches with varying sizes and orientations, the tree trunk is often relatively thicker and more rigid than the branches, while the root systems can vary considerably between species. By schematizing those different components as vertical cylinders, hydrodynamic models may become inaccurate when applied away from the conditions where they are calibrated. The vertical gradient in geometry/biomass can result in different wave dissipation estimations (compared to homogeneous elements along the vertical coordinate). The aim of this project is to provide more accurate tree models that approach reality and to provide better estimations of wave dissipation by mangrove vegetation. Lastly, we would like to establish relationships between geometrical tree parameters and tree properties (such as age or canopy density) to account for naturally occurring variation of trees.

1.2. Objectives

This thesis aims to model the complex, geometrical shape of *Avicennia marina* vegetation. It will also provide insight into the wave dissipation behaviour of other species of mangrove vegetation for which the complex geometrical shape is often neglected or highly simplified in hydrodynamic models. We will achieve the desired result by developing an algorithm that generates three-dimensional geometrical tree models with Python, a programming language. The 3D-models of *Avicennia marina* vegetation will be generated based on a large collection of manual measurements which were performed in the greenhouse of Deltares and empirical relations from previous literature studies. This data will provide the required knowledge to set-up the vegetation structure. We then compare the results with frontal surface area measurements to draw conclusions regarding model validity. In the end, we obtain a distribution of the frontal surface area as a function of the vertical coordinate/height. This information can later be used to determine the rate of wave attenuation in simulations.

Research question
To meet the objective, we formulate the following research question:

How to construct geometrical tree models of Avicennia marina vegetation and how to obtain the projected frontal surface area distribution over the height, $Av(z)$?

Sub-questions
Corresponding sub-questions that must ultimately answer the main research question are:

- Which allometric relations can be used for *Avicennia marina* vegetation?
- How does one define/set-up a geometrical tree model?
- How does one obtain the projected frontal surface area distribution from a geometrical tree model?
- Which effect do the different structural tree parts have on the frontal surface area distribution over the height?
- What are the differences with previous (more simplistic) mangrove schematizations from literature?

1.3. Research scope

The scope of the research must inevitably be narrowed down due to time and the high level of complexity resulting from the interactions between wave hydrodynamics and mangrove vegetation. Ecosystems are highly variable and contain many (ecological) processes at different timescales. For this reason, we restrict the scope of the research to the following situations:

- The research limits itself to mangrove species *Avicennia marina*.

- Dynamic (ecological) processes are not considered (e.g., biotic factors, sediment fluctuations and soil formation and human interventions).
- Only F-type (Fringe) mangrove forests are considered (mangroves exposed directly to incoming wave attack). Other land form types do not have significant incoming wave energy and are therefore outside the scope of this research.
- Leaf geometry is neglected because it is expected that this contributes little to the total frontal surface area of a tree model due to its streamlined shape and high flexibility under wave attack, based on results from van Wesenbeeck et al. (2022).

1.4. Research approach and outline

The research can be subdivided into four main parts that must ultimately answer the main research question. In this section, we elaborate on these parts. The main parts are:

- a literature study
- taking tree measurements in the greenhouse
- a data analysis of tree measurements
- the construction of geometrical tree models

First, we conducted a literature study on general tree structure schemes and characteristics/allometric relations of *Avicennia m.* vegetation. This information was used as input for the computer model but also to get a general understanding of tree structures needed to conduct proper tree measurements in the greenhouse.

Specific parameters were measured, such as branch dimensions, branch orientations, branch distributions and branch relations (diameter ratios between subsequent branches). Four trees with different characteristics were measured in detail to obtain a range of measurements. The trees varied in size (age) and canopy density. From this, estimates can be made of tree models for other tree ages by interpolation or extrapolation of the results.

All measurements were registered by hand and digitally inserted into a tree data structure. We executed the data analysis by creating a search tree algorithm that could loop through all data and output the most valuable results, which we could implement in the tree models. This data includes information on branch dimensions for different branch classes and the distribution of these branches for various tree types.

Lastly, we constructed two tree model types. Both models took on a different approach. Tree model 1 is based on branch ratios and is more deterministic. Tree model 2 is based on branch dimensions that follow probabilistic distributions. Both tree models output the distribution of the frontal surface area over the vertical coordinate Av(z). We compare both tree models regarding this parameter. Consequently, a conclusion follows regarding the applicability of geometrical tree models for hydrodynamic modelling that involves mangrove vegetation.

2

Theoretical background

2.1. Mangrove geometry

Constructing geometrical mangrove models requires understanding of mangrove geometry and tree classification strategies. Mangrove vegetation consists of various tree parts that may or may not interact with waves depending on the height of the water column, namely the tree canopy, -roots and -trunk. The geometry of these tree parts depends largely on tree age and -characteristics. In the following sections, elaborations are described on the structural tree parts, field measurements and established allometric relations for *Avicennia marina* vegetation. An overview of the global distribution of *Avicennia m.* vegetation is shown in Appendix A (Duke et al., 2010).

2.1.1. Root structures

The general root structures of mangrove species *Avicennia m.* are shown in Figure 2.1 (Schiereck, 2012). We only consider *Avicennia m.* mangroves, therefore, only the pneumatophore root structure is of interest for this study. Maza et al. (2017) showed that wave dissipation by mangrove root systems is considerable and must therefore be taken into consideration.

Figure 2.1 illustrates the general root structure of *Avicennia m.* vegetation. *Avicennia m.* has a star-shaped network of cable roots radiating out from the trunk. From these cable roots, anchor roots are shooting downwards and aerial roots, so-called pneumatophores, are shooting upwards (Jordan & Frohle, 2022). It appears that pneumatophores have a conical/cylindrical shape at first glance. Moreover, the cross-sectional base diameters of pneumatophores were measured in the field by Jusoh et al. (2016) and turn out to be in the range of 95 ± 15 mm. Furthermore, pneumatophores have a limited height of less than 30 cm according to field observations by Thampanya (2006) and are more often around 20 cm.

Liénard et al. (2016) measured the diameter decrease over the pneumatophore height at the base, middle and tip-1cm in order to define the pneumatophore geometry.

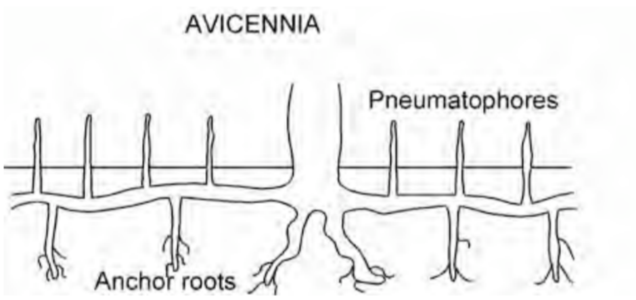

Figure 2.1: Root structure of Avicennia mangroves (Schiereck, 2012).

2.1.2. Trunk diameter

The trunk diameter is often defined by the diameter breast height DBH. DBH is defined as the diameter of the tree trunk at a height of 1.30 m above the substrate or, if the tree is too small, at one third of its height (Horstman et al., 2014).

2.1.3. Avicennia marina measurements and allometric relations from literature

As stated in the introduction, this research limits itself to modelling mangrove species *Avicennia marina*. To this end, only field measurements and allometric relations that apply to *Avicennia m.* vegetation are considered. Table A.2 in Appendix A contains a list of the diameter breast heights (DBH) and heights (h) of thirty *Avicennia m.* tree samples that were measured in the field by Intarat and Vaiphasa (2020) in Bang Pu, Thailand.
According to Intarat and Vaiphasa (2020), *Avicennia m.* trees can grow up to 14 m in height. Figure A.2 shows that naturally occurring mature trees have a height in the order of 10 to 12 meters, whereas the largest vegetation in Deltares' greenhouse reaches up to a maximum height of 2 to 3 meters. The difference in growth stages should be taken into account by translating the outcome in the laboratory situation to the field situation. The largest trees in the greenhouse have been growing for five years approximately, which is still considered a very young tree/sapling according to the definitions by Clarke (1995). An overview of natural growth stages as a function of age is shown in Figure 2.2 and results from research by Clarke (1995). Maza, Lara, et al. (2021) has similar growth stage definitions for mangrove vegetation.
Komiyama et al. (2008) concluded, based on reviewing 72 published articles on mangrove allometry, that the above-ground biomass (AGB) of mangrove vegetation varies with age, type of species and location. One of the reviewed articles by Comley and McGuinness (2005) found an allometric relation for *Avicennia m.* mangroves that relates DBH (cm) to AGB (kg) (equation 2.1). This relation is valid for the range of $DBH's$ up to 35 cm. DBH measurements were executed at a height of 1.30 m above the local ground level. The allometric relation by Comley and McGuinness (2005) was found by sampling 11 trees with 22 stems in total. Thus, (mature) *Avicennia m.* trees can be multi-stemmed. Furthermore, *Avicennia m.* has a wood density of $0.670\, gcm^{-3}$ according to findings by Purwiyanto and Agustriani (2017).

$$AGB = 0.308\, DBH^{2.11} \tag{2.1}$$

with AGB being the above-ground biomass in kg and DBH in cm.

Intarat and Vaiphasa (2020) found that the measured AGB of *Avicennia marina* trees correspond best with the allometric relations as found by Comley and McGuinness (2005). However, this only considers the AGB for one tree stem. An additional allometric relationship was proposed for multi-stemmed mangrove trees by Fu and Wu (2011) that relates above-ground biomass (AGB) to canopy diameter (CD) and height (H) by a linear regression equation (2.2). It does make sense to measure canopy diameter instead of DBH for multi-stemmed trees. *Avicennia m.* is often in between multi-stemmed and single-stemmed in morphology which complicates choosing the right allometric equation.

$$AGB = 1.8247\,(CD^2 * H)^{1.0202} \tag{2.2}$$

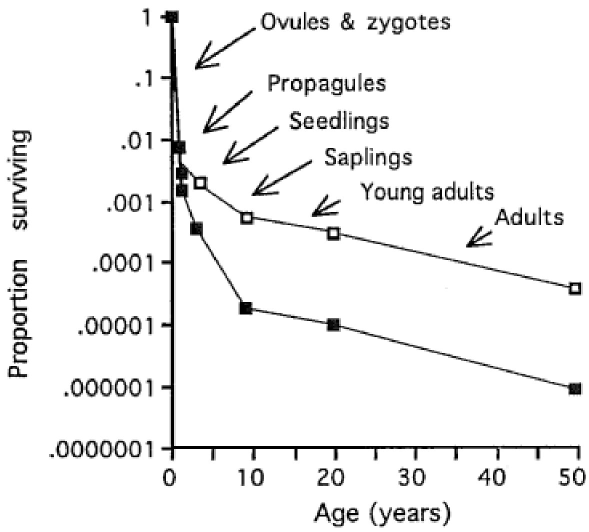

Figure 2.2: Survivorship throughout the life history of Avicennia marina trees (Clarke, 1995)

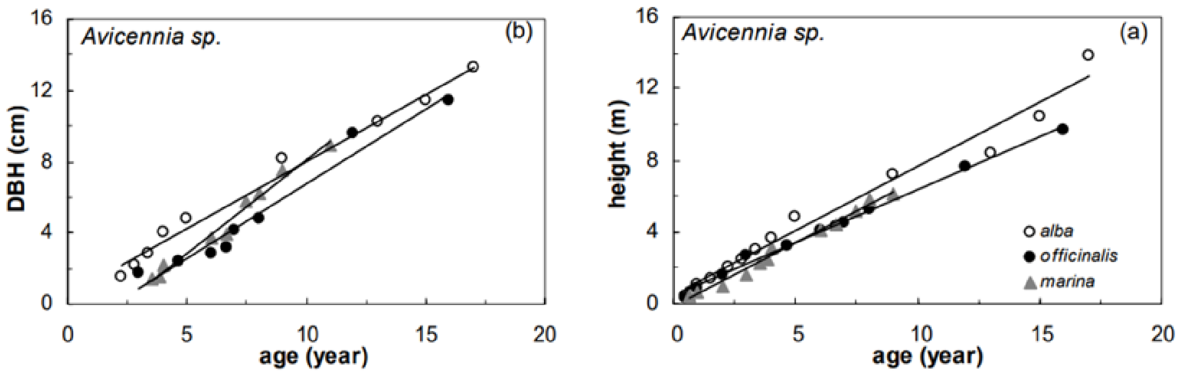

Figure 2.3: Linear regression of three Avicennia species with Avicennia m. being the represented by triangular dots. (a) Height-age and (b) DBH-age (Thampanya, 2006)

2.1.4. Tree ordering schemes

In the past, efforts have been made to come up with a way to describe tree structures in a systematic manner. McMahon and Kronauer (1976) applied an ordering scheme for trees to gain a better understanding of the mechanical design of trees. The ordering system assigns an order to branches ranging from the smallest branches (1st order) to the largest trunk (highest order). Then, several ratios are defined namely a branching ratio R_B, a diameter ratio R_D and a length ratio R_L. These parameters describe the differences between two subsequent orders. The ratios are defined as:

$$R_B = \frac{N_M}{N_{M+1}} \tag{2.3}$$

$$R_D = \frac{d_{M+1}}{d_M} \tag{2.4}$$

$$R_L = \frac{L_{M+1}}{L_M} \approx R_D^{2/3} \tag{2.5}$$

This information can be used to construct a mechanical design with certain measured branch dimensions. Moreover, McMahon and Kronauer (1976) showed that a tree is approximately self-similar, which indicates that a small part of tree is representative for the whole tree structure. A visualization of a mechanical tree structure is shown in Figure 2.4. Additionally, other parameters are needed: d_{min} is the minimum branch diameter (order 1), d_{high} being the average diameter of the highest order (trunk), H being the plant height, L_{high} is defined as length of the highest order and $Nm, high$ is the number of stems rising from the ground. With all these parameters known, one could, in principle, construct a tree structure and estimate the frontal surface area of the vegetation the according to the method as described in Järvelä (2004). Finally, the projected plant area for an order m can be obtained as the product of d_m, L_m and N_m. The summation of all orders M gives the total projected area of the vegetation.

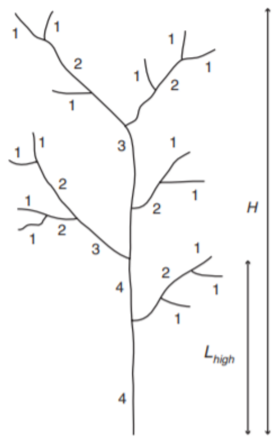

Figure 2.4: Tree structure ordering scheme

The structure of plants can also be described in an algorithmic way using Lindenmayer systems (L-systems) (Prusinkiewicz & Lindenmayer, 1996). The result is a graphical representation of the structure of a plan. It builds upon the notion of self-similarity. Self-similarity relates plant structures to the geometry of fractals. Originally, this theory is applied in the field of computer graphics. L-system structures need certain input parameters such as initial plant structure (axiom) and algorithmic rules regarding geometrical tree growth parameters such as branch developments and angles, which can be measured in the field. Besides, one can also include stochastic processes and vary the degree of randomness.

Previous studies have shown that geometrical tree models are often generated by reconstructing point cloud data (obtained from terrestrial laser scanners) (Intarat and Vaiphasa, 2020; Du et al., 2019; Hackenberg et al., 2014) or from photographs through image segmentation techniques (Shlyakhter et al., 2001). However, these methods only give the geometrical structure of the tree structure that is being scanned/photographed and does not take natural variation into account.

3 Methodology

This chapter explains the methodology used to carry out the manual measurements in the greenhouse. Furthermore, a description of the analysis and storage of data is provided. Also described is the design methodology used to create the geometric tree models. All components that together make up the complete tree model will be discussed in detail. For the individual components (underlying functions of the model), certain choices will be motivated on the basis of theory, practical considerations or observations.

3.1. Measurement methodology

3.1.1. Measurement plan

Table 3.1 lists geometrical tree parameters to be included as input for the geometrical tree models. Most of the parameters originate from literature and determine the shape of the vegetation. The average branch lengths and diameters for each order (smaller twigs up to the highest-order stem) are necessary to create a mechanical tree structure (see Section 2.1.4).

The aim is to measure:

- 2 mature trees (1 dense canopy, 1 sparse/open canopy)
- 2 saplings (shrubs) (1 dense canopy, 1 sparse/open canopy)

The motivation for this selection is that we will be able to generate geometrical tree models for various growth stages (young vs. mature) and various canopy densities (sparse vs. dense). This information allows us to establish relationships between vegetation characteristics and three dimensional shape. The aim was to fully measure the canopy of one large tree (all branches). The smaller trees (saplings) have been fully measured as well. For the remaining tree, only some branches have been measured randomly. However, the branch configuration/structure of every tree will be mapped in detail.

A brief summary of the tree measurements:

- **Branches, including stem**: diameters (variation over the length), lengths, order, amount of side branches for each branch.
- **Pneumatophores**: density, shape, diameter gradient, height.
- **General**: tree height, box dimensions, images.

Table 3.1: Measurement plan - *Avicennia marina* vegetation.

Parameter	Unit	Method
Trunk height	cm	measuring tape/pole
Trunk diameter	mm	caliper/measuring tape
Average branch diameter of orders [m, m+1...M]	mm	caliper
Average branch lengths of orders [m, m+1...M]	cm	measuring tape
Pneumatophore height (μ, σ)	cm	measuring tape
Pneumatophore diameter (μ, σ)	mm	caliper
Pneumatophore density	$\frac{Number}{boxarea}$	counting
Branch angles	$degrees$	protractor/observations
Number of child branches (order m) of mother branch order m+1	-	observations

3.1.2. Selecting trees for measurements and general observations

Trees (or saplings) were selected in such a way that we may ultimately be able to answer the main questions. In the end, relationships must be found between tree properties on the one hand and geometrical properties on the other hand. In addition, differences will be highlighted between tree types. Consequently, the following trees are selected based on their characteristics:

Figure 3.1: Sparse sapling (AV3111 - box 31)

Figure 3.2: Dense sapling (AV3211 - box 32)

Figure 3.3: Dense (young) tree (AV511 - box 5)

Figure 3.4: Sparse (young) tree (AV1211 - box 12)

Table 3.2: Tree characteristics of selected trees.

Tree id	Growth stage	Canopy density	Height
AV511 (box 5)	young tree (5 years old)	dense	1.89 m
AV1211 (box 12)	young tree (5 years old)	sparse	2.46 m
AV3111 (box 31)	sapling (1.5 years old)	sparse	1.07 m
AV3211 (box 32)	sapling (1.5 years old)	dense	0.89 m

Table 3.2 summarizes the main tree characteristics of the selected trees. As a general observation, all trees were partly pruned which affects measurements which may cause differences between greenhouse trees and naturally occurring trees. However, pruning was not done excessively. In addition, tree types AV3211 and AV511 have a more complex branch configuration at first sight compared to tree types AV3111 and AV1211.

3.1.3. Execution of root measurements

Several parameters were measured to capture the geometrical shape of pneumatophores. The height (*h*), base diameter (D_b *or* D_{0h}), diameter halfway (D_m or $D_{0.5h}$) and top diameter (D_t or $D_{0.9h}$). The tip diameter (D_{tip}) is set to zero. A visual representation of these parameters is shown in Figure 3.5. A total of 100 roots were measured, 25 roots per tree (open sapling, dense sapling, open tree and dense tree).

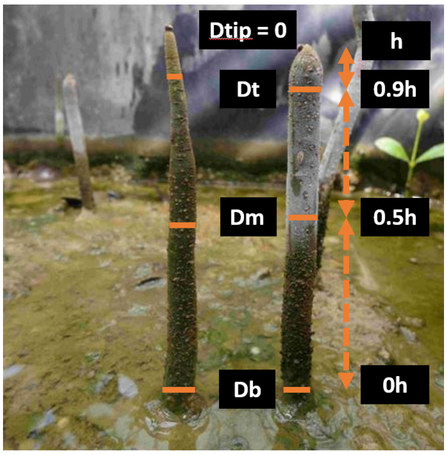

Figure 3.5: Measured root parameters and natural variation between roots

Figure 3.6: Natural variation of root shapes

3.1.4. Execution of canopy measurements

When mapping the canopy structure, first visual observations were made to determine the configuration of the tree. The growth of a tree is determined by many factors such as light, humidity, space, pruning and nutrients to name a few. All of these factors will be neglected for the construction of the model. From observations followed that some similarities occurred between trees in terms of branching configuration.

An effort has been made to draw the complete canopy structure (branching pattern) for each tree and, thereafter, collect the branch measurements in this drawing. This has proven to be helpful and it minimised the risk of incorrect measurements because by using the drawing, one can keep track of the current position within a tree structure. The large number of branches can quickly lead to confusion and disorder. Examples of such drawings containing branch patterns and branch dimensions can be found in Appendix C for the sake of illustration.

3.2. Data storage and analysis

The goal of the manual measurements is to discover the structures of vegetation types that vary in size, life stage and biomass density and to establish relationships accordingly. Moreover, the relationships between branches of different order will be useful for geometrical modelling. The measurements also allow us to validate if the notion of self-similarity holds for *Avicennia marina* vegetation. The concept of self-similarity has shortly been explained in Section 2.1.4 and may ease the construction of an algorithm that describes tree structures.

3.2.1. Tree data structure

The data on branch structures is stored in a tree diagram format. The motivation for this choice is that the complex relations between branches can best be described in a tree-like data structure, which is a hierarchical, non-linear data structure. With this tree data structure, it is possible to distinguish subsystems (side branches) from the largest system (whole tree). The tree data structure consists of a root node (which is the tree trunk), nodes and edges. Each node contains information of the branch such as its order (O) according to the tree-ordering system as defined in Section 2.1.4, branch diameter (D), branch length (L) and branch height [H). The collection of nodes forms a network of branching patterns which are connected by edges. Edges are a way to describe so-called parent-child relationships. In other words, a child branch of a parent branch is synonymous for a side branch which branches of from a main branch. Consequently, one can deduce relationships from this network which, in the end, will be used as input for our geometrical model. A graphical representation of the tree data structure is shown in Figure 3.7.

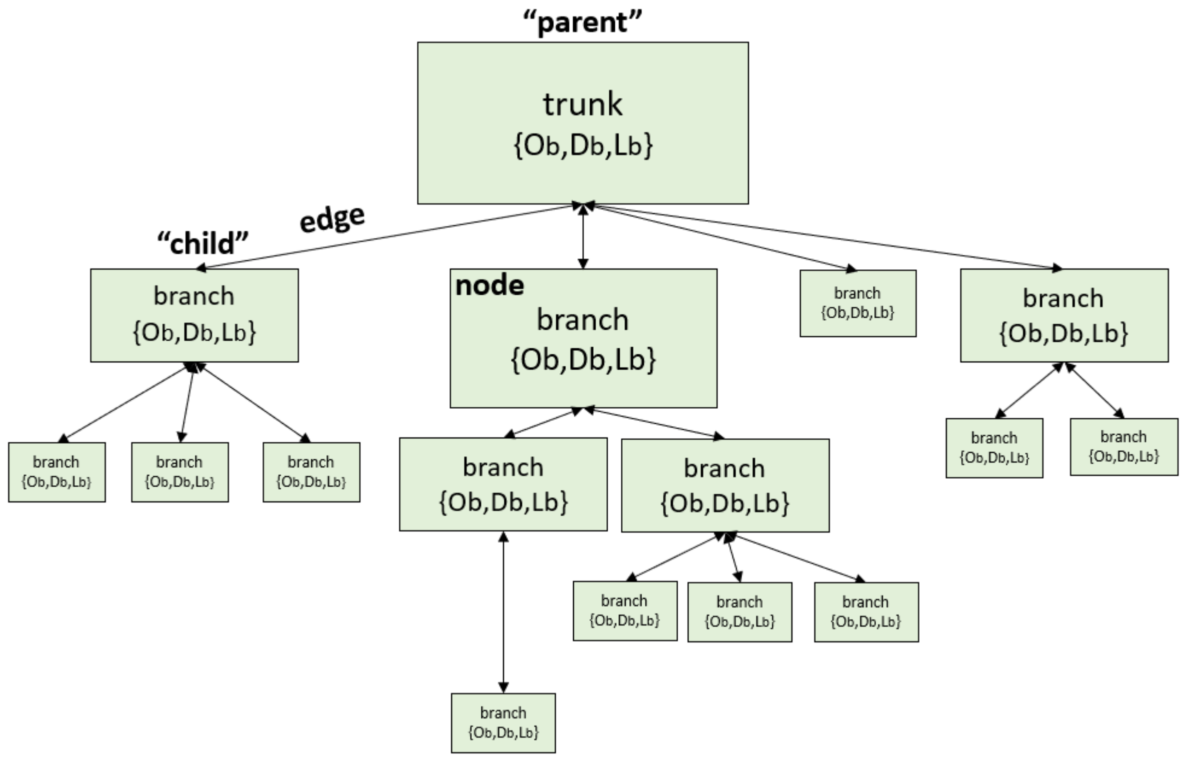

Figure 3.7: Tree data structure for data storage of branch properties: branch order (Ob), branch diameter (Db), branch length (Lb) and parent-child relations

The chosen data structure is implemented in Python by using so-called "Classes". A class is created prior to the introduction of any data and we named the class "treenode". A Class is like an object constructor, or a "blueprint" for creating objects. It consists of properties and values can be assigned to these properties. In our case, the properties were order, diameter, length and height (above the ground). Consequently, the object that is being defined is a branch. This procedure is repeated for every branch of the four considered tree systems. The power of this method is that properties of a certain object can easily be recalled and stored. Moreover, one can assign relationships between certain objects (tree nodes), these are the parent-child relationships that we mentioned earlier. All values are stored within the file: "Datafile_Mangroves".

3.2.2. Analysis of canopy measurements

After inserting all data points, the data was analysed. This was done by using a "non-binary search tree algorithm". This is an algorithm that starts at the top of the tree (see Figure 3.7) with the highest order branch (the trunk) and works its way down to the branches which are connected to it. Then the process repeats itself by looping through all nodes. During this process, several computations are executed between subsequent nodes regarding diameters and ratios. These values are then being stored in data arrays. It may be difficult to visualize this process and, therefore, Figure 3.8 serves to support the explanation given.

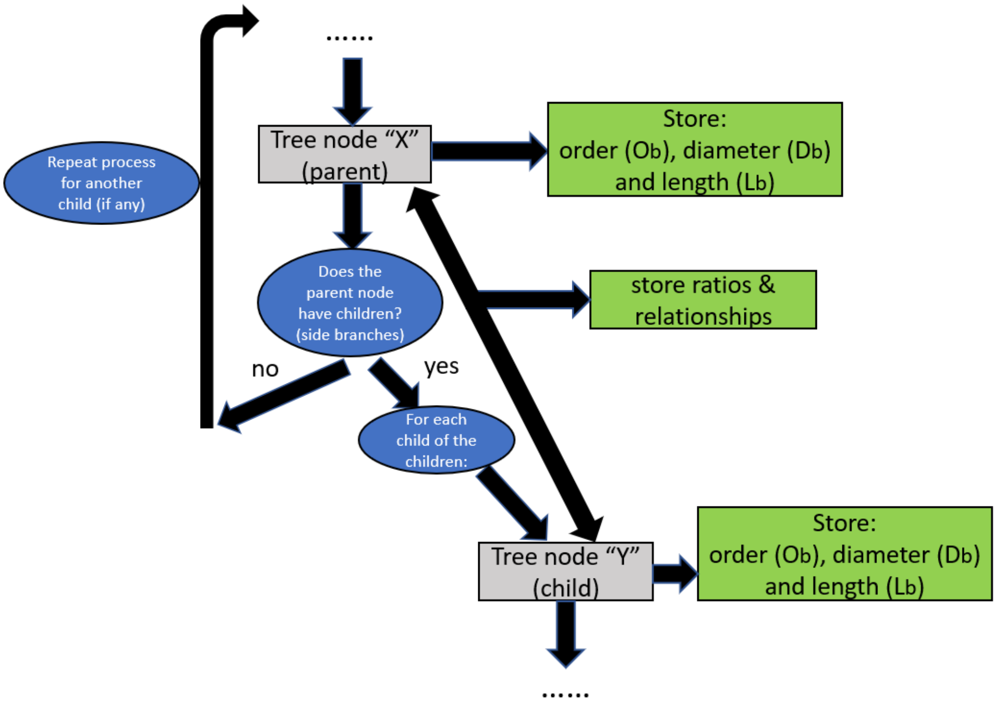

Figure 3.8: A non-binary search tree algorithm visualization that stores branch properties branch order (Ob), branch diameter (Db), branch length (Lb) and parent-child relations (diameter ratios and branching configurations)

Part of the Python code for the algorithm can be found in Appendix D and gives an impression of the steps for the data storage and -analysis. Firstly, the definition of the class "treenode" and secondly a part of the search tree algorithm. The search tree algorithm can be called from every tree node.

The aim of the search tree algorithm was to give the following output for each branch order M (with M-1, M-2 etc.. being smaller order branches):

- quantity
- mean diameter and standard deviation of the diameter
- mean length.
- average number of total side branches
- average number of side branches of order M_{-1}, M_{-2}...
- average diameter ratios D_M/D_{M-1}, D_M/D_{M-2}, etc..

A data frame is set-up to provide all the above-mentioned values. Additionally, the mean diameter for each order is plotted against its mean length. As a result, a relation is obtained between branch diameters and branch lengths through empirical curve-fitting. The curve fitting process is executed in Excel and, depending on the type of tree, a relation was found that will be used for the construction of the geometrical model of a particular tree type.

3.3. Tree model construction

The model is made up of several parts that together form the whole tree structure. First, the set-up of the root model (pneumatophores) is discussed (Section 3.4). Second, the set-up of the canopy models will be explained in Section 3.5. We created two different canopy models that will be explained in detail.

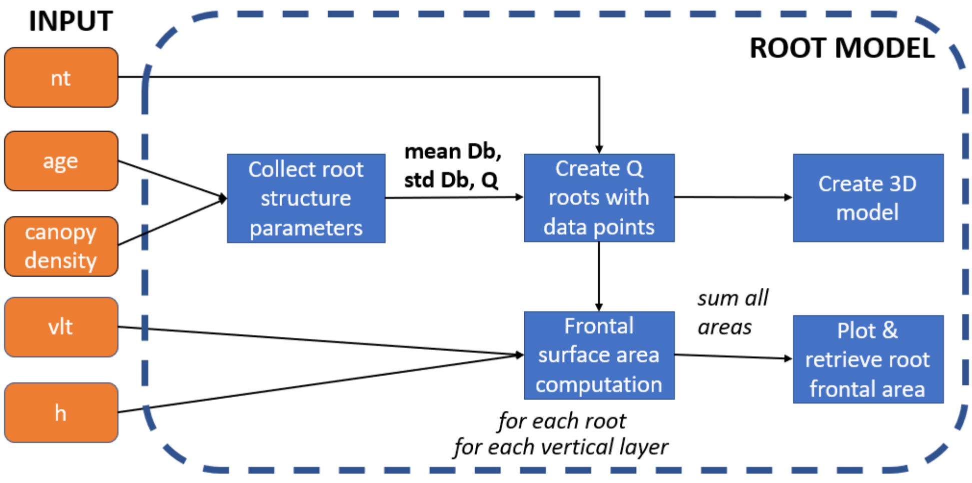

Figure 3.9: Root model schematization

3.4. Root model construction

The goal was to construct a geometrical root model for a variety of trees depending on age and canopy density. Moreover, we sought to know the frontal area distribution over the height because this is used for modeling wave dissipation by vegetation. We started of with the input values that need to be defined before running the model:

1. **nt**: a precision parameter that determines how many data points will be created for the geometry of a root. If nt is high, more data points are generated and the geometry of the roots will be smoother. However, this will be more computationally demanding.
2. **vlt**: stands for "vertical layer thickness"; the frontal surface area of the root will be computed over distinct layers with length "vlt" expressed in mm.
3. **H**: stands for the maximum height that is considered within the frontal surface area plot. H is expressed in mm.
4. **tree age and tree canopy density**: both combined define the type of vegetation. This could be "Open sapling", "Dense sapling", "Open tree" or "Dense tree". This input value is needed to obtain the mean root base diameter (μ_{Db}), the standard deviation of the root base diameter (σ_{Db}) and lastly, the quantity of roots for a given tree type, Q. The geometrical structure of the roots is defined by these parameters.

A schematic overview of the complete root model is shown in Figure 3.9. Note that the root model consists of multiple functions, each of which has a share in the total computation. We will elaborate on all parts within the model.

The geometry of an individual root is based on a certain set of rules in a prescribed order, namely:

- The location of a root is arbitrarily chosen, but within the limits of the box dimensions.
- The base diameter of the root is defined based on the normal distribution that belongs to a certain tree type and followed from the root measurements in the greenhouse.
- The root height is defined based on the root base diameter, according to Figure 4.1.
- The diameter decay over the root height is based on the root height, according to Figure 4.3

If and only if the base diameter (D_b), height (h), location ((x, y) and diameter decay of the roots are known, then it is possible to construct the root geometry and obtain the frontal surface area distribution. Therefore, determining these parameters is an important step that is performed by the root model.

A large part of the code is the creation of 3D meshes that define the geometrical shape of the tree roots. Some information is provided below to get familiar with the terminology for 3D mesh generation. All the data points are created in the "second blue box" of Figure 3.9 by two functions. The first function computes all x,y and z coordinates of the vertices. The second function returns arrays with identification numbers of vertices. In the next sections, the methodology of creating 3D models is explained in more detail and it stresses the importance of defining vertices. The same procedure is followed in our root model. Finally, the computation of the frontal surface areas of the roots will be explained.

3.4.1. Generating 3D meshes for geometrical objects

In the field of computational geometry, a number of terms are vital for the construction and understanding of geometrical models. We limit ourselves to three terms and their definitions: vertices, edges and faces.

Vertices are corner points of a 3D model that are connected to each other by edges. Edges are thus lines that connect vertices. Faces are flat surfaces of a model. An edge is where two faces meet and, therefore, separates two faces from each other. Figure 3.10 shows the vertices, edges and faces of a root model (not to scale for demonstrative reasons) to endorse the provided explanation.

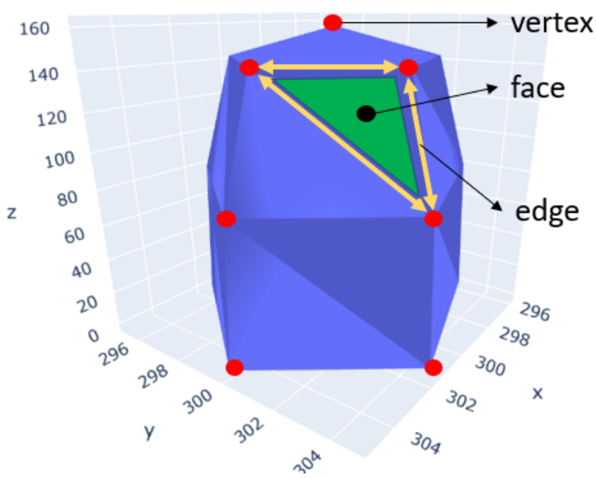

Figure 3.10: Visualisation of vertices, edges and faces of a 3d mesh model. nt is

The "go.Mesh3D" function in Python can construct 3D meshes based on Cartesian coordinates (x,y,z) and vertex numbers (i,j,k). Vertices are assigned a number and one combination of i,j and k data points forms a triangle, which is a face. Therefore, the 3D model is the total combination of triangles. Triangulation is the process of obtaining a mesh (from data points) that consists of a large amount of triangular faces. The "go.Mesh3D" function can be executed to start the triangulation given a set of x,y,z,i,j and k data points.

Two functions were written to account for the vertices of a root shape (pneumatophore) and a branch shape. The latter is needed for constructing 3D models of branches.

3.4.2. Root frontal surface area computation

One of the research questions was to find out whether root systems, such as pneumatophores play a significant role in wave attenuation estimations. Because of this, an algorithm has been written to compute the distribution of the frontal surface area over the height. Because the size and shape of the protruding roots can vary quite a bit, the approaching surface of each root must be calculated separately. Figure 3.11 shows two different roots, varying in size. The larger root will have a larger frontal surface area over the height and therefore will contribute more to wave attenuation compared with the smaller root on the left. The distribution of the frontal areas over the height depends on the chosen value of the vertical layer thickness (vlt). If vlt is very large, then the summation of frontal surface areas of all roots will be assigned to the first layer.

The frontal surface area of a root has been computed in the following manner. Firstly, the locations of the root tip, root top and root middle were determined. Secondly, the root diameter decay of root sections base-middle, middle-top and top-tip have been determined. Thirdly, one has to account for various cases because the tip, top or middle locations could be present within one vertical layer or spread across several layers. For example, by looking at the small root of Figure 3.11, one can notice that the root tip and top are located within one layer. Furthermore, the vertical layer is not fully covered by this root because the tip is lower than the upper limit of the vertical layer. The diameter decay may also vary within a layer, depending on the root height. All of these issues have been taken into account by creating eight different cases that may occur for the distribution of the root areas over height depending on the chosen vertical layer thickness.

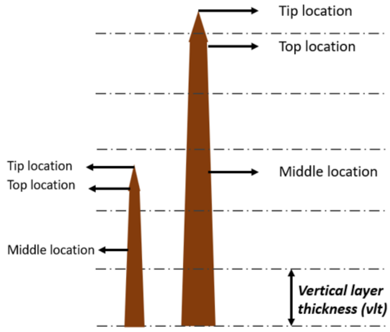

Figure 3.11: Two schematic roots and a visualization of their shape/frontal area that is distributed over various layers with a certain thickness (vlt)

.

The result of the computation is an average root diameter for each vertical layer, which is then multiplied by the vertical layer thickness (vlt) to obtain the frontal area. Thereafter, the sum is taken of all roots to obtain the total frontal surface area. We neglect shielding effects that might occur for roots that are located in close proximity of each other.

The frontal surface area distribution is represented by a step plot. One can indicate the desired total height to be shown (H) and the vertical layer thickness, vlt.

3.5. Canopy model construction

The canopy of a tree consists of many branches that vary in size and orientation within a certain tree volume area. A challenge in constructing branch systems is that the properties of a side branch depend partially on the properties (size and orientation) of the branch from which it originates. The model design can take into account these complexities and, as a consequence, a systematic approach is crucial for the success of the geometrical model. The canopy model consists of multiple functions that each serve a certain purpose. We elaborate on each of these functions in the following subsections, starting with functions that create a single branch geometry. As we continue, the complexity gradually increases towards the construction of a system of branches. A schematic overview of the canopy/branch system model construction process is shown in Figure 3.12. We construct two canopy models that each follow a different systematic approach of constructing branch geometries within the canopy system. The different approaches are explained in Section 3.5.1 . Lastly, we explain how the root model and canopy are merged to obtain the full tree model.

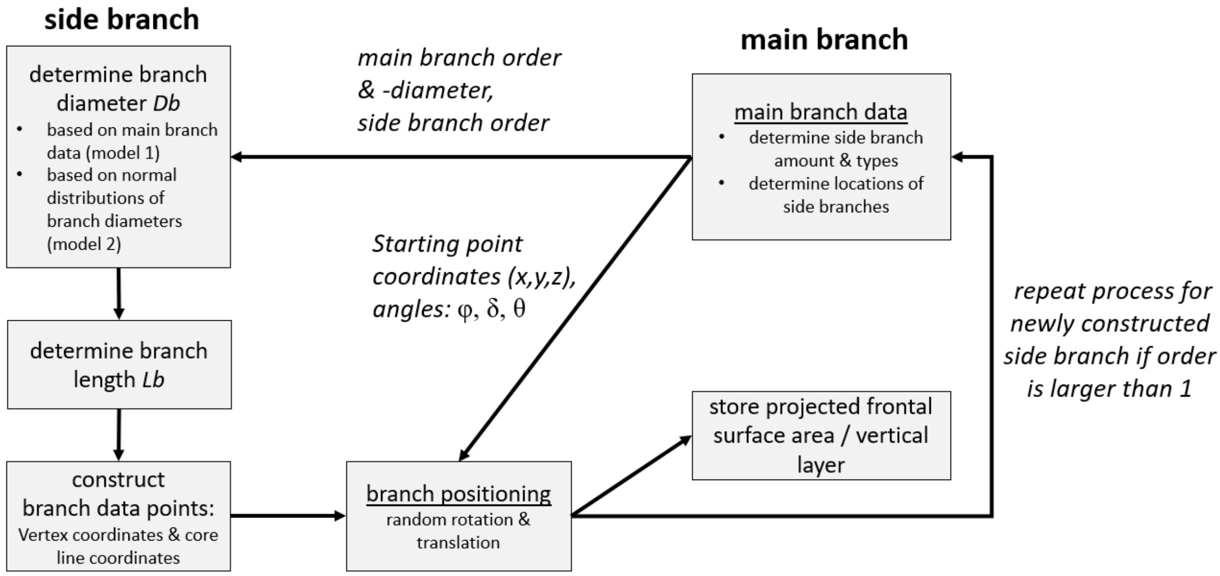

Figure 3.12: Schematic overview of the repetitive branch construction process (canopy model). Each arrow indicates a data stream.

3.5.1. Individual branch geometry set-up

The construction of a (side)branch starts with the information input from the main branch. An initial value for a branch diameter is provided by the model in the absence of a mother/main branch, which is the case for the tree trunk. The initial value for the diameter of trunk (highest order branch) follows directly from allometric relations that originate both from literature (see Section 2.1.3 and measurements (see Section 4.1.2. In all other cases, the branch is preceded by the construction of a main branch and, consequently, information travels from the main branch to the side branch.

The process initiates at the main branch. We determine, based on the main branch characteristics, how many side branches it will have. The average amount of side branches for each branch order and each tree type is stated in Table 4.2, 4.3, 4.4 and 4.5 of Section 4.1.2. Not surprisingly, this value is not an integer since this is the average of all branches of a certain order. We can only construct an integer amount of side branches. To facilitate this, every side branch count of every main branch has been stored in assigned data arrays. The mean value of this array is equal to the listed value in the above-mentioned Tables. Consequently, one obtains a record from which we can randomly select the amount of side branches. A record will be in the following format:

$$A_{no.sidebranches/orderM/treetype} = [2,4,2,3,7,5,2,3,2,2,5,4,2,2,2] \tag{3.1}$$

If we would randomly select an index value of the example array from Equation 3.1, then the probability of occurrence of two side branches, $P(sidebranches = 2)$ becomes 0.533 or 53.3% while for the case with seven side branches, $P(sidebranches = 7)$ becomes 0.067 or 6.67%. Thus, it is more likely that the main branch contains two side branches instead of seven. The observations of varying side branch amounts clearly demonstrate the random/probabilistic nature of tree structures. Introducing this methodology account for this aspect. Note that the amount of side branches of a main branch cannot be lower than two as this would contradict the branch ordering system. Additionally, branches of order one will not have side branches. As a result, the process will stop by breaking the loop.

Apart from knowing the amount of side branches, we must also determine the branch order class of the intended side branch to construct the branch geometry and further develop the complete branch structure. Again, we have stored all side branch order for each main branch order for each tree type, resulting in even larger data arrays. We again use the random selection technique to account for variation in branch order classes. For the sake of illustration, Array 3.2 demonstrates the variety in side branch order classes for the main stem (branch order 6) of a dense tree (AV511 (box 5)) with twenty side branches.

$$A_{sb-orders/O6/dense-tree} = [5,5,4,3,2,5,4,3,2,3,2,1,3,2,1,4,3,2,3,2] \tag{3.2}$$

However, one should be careful when applying this methodology. A branch of order M must in all cases contain at least two side branches of order $M-1$. With the random selection from Array 3.2 one might miss these values which will result in an incomplete, unrealistic tree model that is not in line with the intended systematic approach. Therefore, two values of order M-1 (order 5 in this case) are removed from Array 3.2 and will always be part of the collection of side branches. This methodology is always applied to retrieve a correct tree model in a theoretical sense. We arrive at the (side) branch construction part (the left part of Figure 3.12 when the side branch type is known. We make a distinction between two systematic approaches for the construction of the branch geometry: model 1 and model 2. We will now explain each model in detail.

Model 1 - deterministic approach for determining branch diameter D_b

The first canopy model takes dependency and relations between branches into account for determining the branch diameter. In a way, the model is deterministic because it assumes causal relations between branches. Three factors influence the diameter of an intended side branch, namely:

1. main branch order, order M (branch from which it originates)
2. main branch diameter, Db_M (branch from which its originates)
3. side branch order of branch to be constructed, random choice of order: $[M_{-1}, M_{-2}, M_{-3}, ..., 1]$ (determined according to the probabilistic distribution of main branch order type).

The above-mentioned data travels from the main branch to the respective side branch. With both branch orders and the main branch diameter known, one is able to compute the branch diameter of the side branch. The average ratios of the main branch diameter (order M) and side branch diameter (order $M_{-1}, M_{-2}, M_{-3}, etc..$) have been computed through data analysis (see Section 3.2.2) and the results are listed in Section 4.1.2, Tables 4.2, 4.3, 4.4 and 4.3 for respectively an open/sparse sapling, dense sapling, open/sparse (young) tree and dense (young) tree. The results are implemented in model 1. One obtains the side branch diameter by dividing the main branch diameter with the found ratios.

Model 2 - Fully probabilistic approach for determining branch diameter D_b

For the second type of canopy model, every branch diameter is generated based on the normal distributions of branch diameters for each branch order. This method does not take dependencies between subsequent branch connections into account. However, it does take into account natural variation of branch diameters and, consequently, branch lengths (for a branch order class) due to the probabilistic approach. For example, an order one branch can be assigned a branch diameter of 2 mm but it could also be 4 mm. The mean branch diameter (μ_{Db}) and branch diameter standard deviation (σ_{Db}) for each branch order class have been determined through analysis of the measurement data. The normal distribution parameters can be found in Section 4.1.2, Tables 4.2, 4.3, 4.4 and 4.5 for the measured tree types and were determined in Python.

3.5.2. Branch length derivation

Using either model 1 or model 2, a branch diameter is obtained. A trend was discovered between branch diameter and branch length and this is applied in the tree models. The results are displayed in Section 4.1.2.

3.5.3. Branch geometry construction

One is able to construct the branch geometry if and only if D_b and L_b are known. That is because D_b and L_b define the dimensions of the branch. We model the individual branches as cylinders. Some time has been spend to investigate the effect of branch diameter decay but no clear relationship could be found. In other words, the gradient of branch diameter decay over the branch length shows demonstrably large variety in results. Therefore, we omit the effect of diameter decay (and thus branches with truncated cone shapes) for now.

The geometry of a branch is constructed in a similar manner as the root structures. Each branch is first constructed at the origin [0,0,0] according to the provided dimensions D_b and L_b. At a later stage, we rotate and translate the branch to the right location (see Section 3.5.4). To this end, we create vertex points. These vertex points (coordinates) are fundamental for the construction of a 3D mesh/geometrical model. The value for nt is a precision parameter and this defines the amount of vertices that the model creates. Similar to the root model, a high value of nt yields more data points and, consequently, a more detailed 3D model, although this comes at the expense of more computational time. The vertex points of a tree model are stored in large data sets, which will be used to create a model in the end by applying a triangulation algorithm. The branch positioning procedure will now be explained in detail.

3.5.4. Branch positioning

A rather challenging aspect of creating a canopy model for vegetation is the accurate positioning of branches within 3D space. In order to facilitate an accurate connection of branches and, to prevent the occurrence of "floating" branches, a "core line" is generated for each branch. The core line exists only for the purpose of defining branch starting positions and computing branch frontal surface areas. A branch structure visualisation is shown in Figure 3.13 and contains a main branch or "mother branch" with side branches (or "child branches") and their respective core lines.

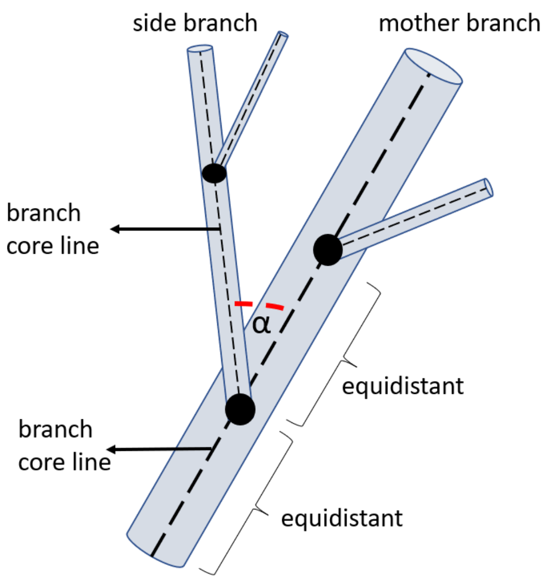

Figure 3.13: visualisation of the side branch positioning process along its main branch.

Rotation

The branch positioning process starts with a rotation of the branch such that it attains the right orientation within the canopy structure. Hence, we implement a rotation function that rotates all x-,y- and z coordinates of branch data points. The rotational transformation function is shown in Figure 3.3 and consists of three rotations, performed in a fixed order through matrix multiplication by rotation matrices R_x, R_y and R_z respectively (see equation 3.4). Note that the model rotates all data points around the origin, therefore, a translation must be performed afterwards to position the coordinates at the right location (see Section 3.5.4).

$$\begin{bmatrix} x_r \\ y_r \\ z_r \end{bmatrix} = R_z(\theta)R_y(\delta)R_x(\phi) \begin{bmatrix} x_0 \\ y_0 \\ z_0 \end{bmatrix} \tag{3.3}$$

With:

$$R_x(\phi) = \begin{bmatrix} 1 & 0 & 0 \\ 0 & \cos\phi & -\sin\phi \\ 0 & \sin\phi & \cos\phi \end{bmatrix}, R_y(\delta) = \begin{bmatrix} \cos\delta & 0 & \sin\delta \\ 0 & 1 & 0 \\ -\sin\delta & 0 & \cos\delta \end{bmatrix}, R_z(\theta) = \begin{bmatrix} \cos\theta & -\sin\theta & 0 \\ \sin\theta & \cos\theta & 0 \\ 0 & 0 & 1 \end{bmatrix} \tag{3.4}$$

First, all branch coordinates rotate around the x-axis by matrix multiplication with R_x given an angle ϕ, which yields new coordinates (x,y,z). Subsequently, the new branch coordinates rotate around the y-axis by matrix multiplication with rotation matrix R_y given an angle δ, resulting again in new coordinates for x,y and z. Lastly, the updated coordinates rotate around the z-axis by matrix multiplication with rotation matrix R_z given an angle θ. As a result, all branch coordinates have rotated with angles ϕ, δ and θ. The combination of these angles are stored by the model and define the orientation of the branch in the canopy structure. Storing these angles is necessary for further positioning of side branches (child branches) as these depend on the position and orientation of their "mother" branch. One can see from Figure 3.13 that a side branch orientation is defined by the orientation of the mother branch plus or minus an angular deflection α. This angle α serves for illustrative purposes. In reality, the model account for three angular deflections for rotations (in degrees) around the x-axis, y-axis and z-axis respectively. Angles ϕ, δ and θ represent the orientation angles of a branch and are defined as the angles of the main branch plus an additional, random rotation within a certain range.

Figure 3.14: Even distribution of side branches along the main branch length

Figure 3.15: 90 degree angle of primary side branches (first side branches from the stem

We distinct between the angles of side branches that originate directly from the stem (further referred to as primary side branches) and all other side branches. The reason for this is the observation of perpendicular angles of ”primary side branches” with respect to the tree stem. This phenomenon is shown in Figure 3.15 and occurs mainly for larger trees and to a lesser extent for saplings. It is uncertain whether the occurrence of perpendicular angles is natural or a result of the conditions in the greenhouse. Either way, we account for this in our particular tree model. The model is created such that angles can easily be modified. Consequently, primary side branches have a ϕ of 90°, δ equal to 0° and θ a random value between 0° and 359°, which is in line with tree observations. Furthermore, one can observe from Figures 3.14 and 3.15 that primary side branches branch off in pairs with opposing directions. This is also taken into account by the model.
We model secondary side branches such that their orientation can rotate up to a maximum value of 60° around each axis, compared with the main branch from which it originates. This is an estimation based on observations of the branching structure. Additional deflections (rotations) larger than 60° for a certain direction (compared to the main branch direction) are rare and give oddly shaped branching structures. In short, the new orientation a side branch order m (with main branch order M) follows from equations:

$$\phi_m = \phi_M + random(-60°, 60°) \tag{3.5}$$

$$\delta_m = \delta_M + random(-60°, 60°) \tag{3.6}$$

$$\theta_m = \theta_M + random(-60°, 60°) \tag{3.7}$$

Translation
One needs to translate the rotated side branch into the right position within the 3D coordinate system, we determine the base coordinates of the side branch by using a dedicated function that creates interval points along the longitudinal axes of the main branch based on the total amount of side branches of the main branch. This results in an even distribution of side branches along the main branch length. Two side branches of order M_{-1} are always placed at the end on a (main) branch order M. For example, a branch with six side branches will have two side branches at $0.33L_b$, two side branches at $0.67L_b$ and two branches at L_b. Let's name the coordinates of a branch starting position sx, sy and sz. Then the translation of all branch coordinates x_0, y_0 and z_0 becomes (equation 3.8):

$$\begin{bmatrix} x_t \\ y_t \\ z_t \end{bmatrix} = \begin{bmatrix} x_r \\ y_r \\ z_r \end{bmatrix} + \begin{bmatrix} sx \\ sy \\ sz \end{bmatrix} \tag{3.8}$$

With: x_r, y_r and z_r being branch coordinates after rotation, x_t, y_t and z_t being branch coordinates after rotation and translation and sx, sy and sz being the start position coordinates on the main branch core line.

3.5.5. Projected frontal surface area of a branch in 3D space

This section explains the methodology for the frontal surface area computations of the branches. Figure 3.16 shows a figurative branch in 3D with starting point (point 1) and end point (point 2). The projected frontal surface area may be different for different planes of orientation. We consider two plane projections: xz-plane and yz-plane. Figure 3.16 shows both viewpoints with respect to the branch.

One needs to find the projected length of a branch Lxz_{branch} or Lyz_{branch} to be able to compute the frontal surface area Ap_{branch}. Hence, one needs to compute the distances dx or dy (depending on the plane of interest) and dz of starting- and end point and, apply Pythagoras' theorem to find the projected branch length. The branch shown in Figure 3.16 is directed upwards but the same procedure holds for branches with a downward or horizontal direction.

One arrives at the situation as depicted in Figure 3.17 when the projected branch length has been found correctly. The total projected branch area Ap_{branch} is then simply calculated as L times D_b. However, Ap_{branch} must be divided over vertical layers with length vlt (see Figure 3.17). To this end, an algorithm has been developed that computes the branch length within a layer (dL). Subsequently, a fraction of the total projected frontal surface area is assigned to the layer of interest. Each area fraction of each branch is stored for each vertical layer. The result is a summation of all branch areas for each layer. The frontal surface area computation is verified by comparing computational results with manually derived solutions for various branch orientations.

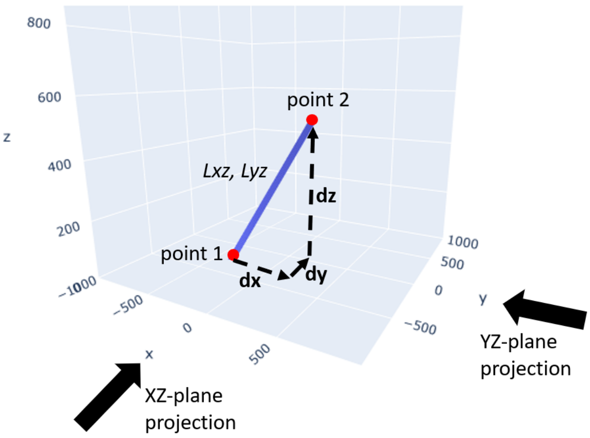

Figure 3.16: Computation of projected frontal surface area of a branch in 3D space

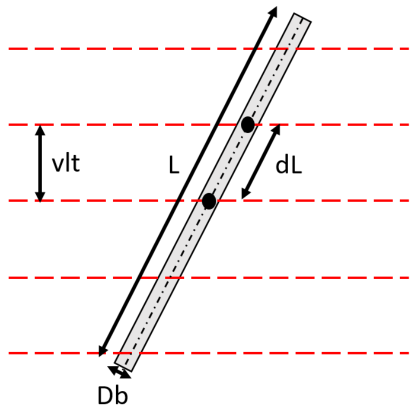

Figure 3.17: projected branch area for plane of interest

4 Results

This chapter summarizes the main findings that result from the manual measurements, which were performed at the greenhouse of Deltares. Subsequently, the results are processed in the model to create a blueprint for generating 3D tree models. The tree models are also discussed in terms of results and validity. This chapter is subdivided into different sections:

- a section dedicated to the results of pneumatophore measurements for various trees (section 4.1.1)
- a section with results of the canopy measurements (branch systems)
- a section that evaluates tree model output results and validation.

4.1. Measurement results

4.1.1. Pneumatophores

The geometry of 100 roots has been fully mapped by performing manual measurements as described in Section (3.4. Twenty-five roots were measured for each of the four trees/shrubs. Both the total height (above ground surface) and the diameter course over the root height were measured for each root. This section aims to describe the results that follow from the root measurements. The main findings were implemented into the geometrical root model which together with the canopy model forms the full tree structure.

All root measurements are listed in Appendix B. The base diameter of a pneumatophore is defined as D_{0h} (namely the diameter at zero height), therefore, D_{0h} and D_b are equivalent. The same holds for $D_{0.5h}$ & D_m and $D_{0.9h}$ & D_t, which are also synonymous. Assuming a normal distribution of root diameters, we obtain Table 4.1 with parameters root mean diameter (μ) and standard deviation (σ):

Table 4.1: Normal distribution parameters for pneumatophore base diameters, for different tree types

tree type	μ_{Db} [mm]	σ_{Db} [mm]	root quantity/box
open sapling (AV3111)	9.55	1.42	31
dense sapling (AV3211)	7.88	1.30	100
open tree (AV1211)	9.46	1.71	246
dense tree (AV511)	8.57	1.85	149

We will use the values from Table 4.1 as input for the construction of the geometrical root model. Later in this chapter, we will demonstrate the correlation of the root height to the root base diameter.

Furthermore, from Table 4.1 can be concluded that the mean root base diameter for dense vegetation is lower than for sparse/open vegetation. However, the values are comparable. The standard deviation for trees is higher than the standard deviation for saplings. Observations in the greenhouse confirm that larger trees contain more outliers in both pneumatophore height and base diameter (higher maxima and lower minima). Therefore, the results are in line with the observations in the greenhouse.

The amount of roots strongly varies between tree types (see Table 4.1. The ”open” tree contains most roots within its limited box dimension space and is also the largest tree of the four trees considered ($\approx 2.50m$). The dense tree has less pneumatophores but the height is significantly lower compared to the open tree (1.90 m). Therefore, it is hard to draw conclusions based on the observations for the trees. Interestingly, the saplings (which are of comparable height) show a large difference in the amount of pneumatophores. The dense sapling has three times as many roots as the open sapling. This leads us to believe that a higher biomass density results in a higher pneumatophore density, which sounds plausible.

Now that we know the data for the base diameters of the roots, it may be interesting to investigate whether the root base diameter is related to the root height. Therefore, the heights of all roots have been plotted against their base diameters. No distinction is being made between tree types. One can see in Figure 4.1 that a trend/correlation is present between the base diameter and height of a pneumatophore. On average, a larger base diameter will result in a pneumatophore with larger height. However, note that this not always the case since random, natural variations will always occur. The trend line used to capture the relation between diameter and height is linear and we will implement the resulting curve fitting line in our geometrical model to determine the root height based on a root base diameter (drawn from the normal distribution). For completion, the base diameters versus root heights per tree type have also been plotted and can be seen in Figure 4.2.

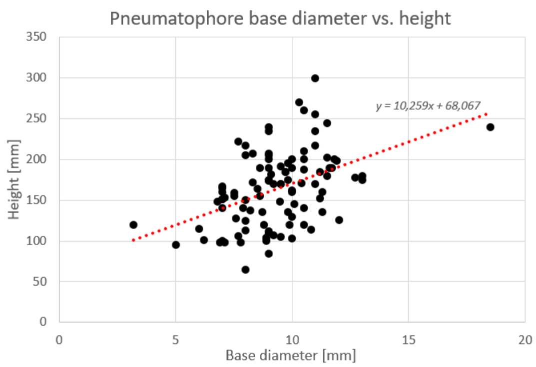

Figure 4.1: Pneumatophore base diameter vs. height (all roots considered)

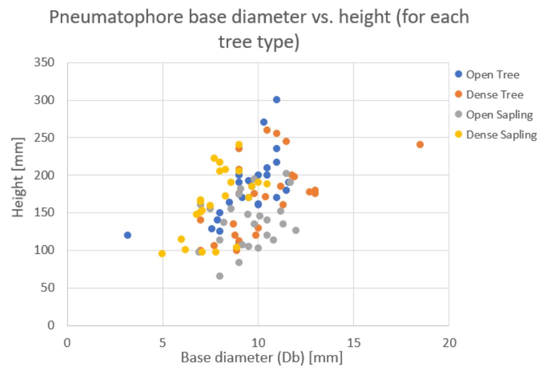

Figure 4.2: Pneumatophore base diameter vs. height (sorted by tree type

Pneumatophore diameter decay over the height

From observations in the greenhouse & and photos (see chapter 3) follows that the root diameter over its height varies along the vertical coordinate. For this reason, we measured the diameter at zero height (D_{0H}), the diameter halfway the root ($D_{0.5H}$) and the diameter at the top (0.9H - $D_{0.9H}$) for each pneumatophore. Consequently, ratios have been determined as described in Chapter 3 - Methodology. An overview of the results is shown in Figure 4.3. The ratios $D_{0.5H}/D_{0H}$ and $D_{0.9H}/D_{0H}$ are plotted for each pneumatophore as function its height, with red dots and blue dots respectively. As a result, one obtains factors that describe the diameter decay along the vertical coordinate of the root. By linearly curve-fitting the results, one can see that, on average, the diameter decay will increase for higher pneumatophores. Therefore, The geometry of small roots will generally be more cylindrical while larger roots will be more conical. We will implement these relations in the model to estimate the geometrical shape of the roots.

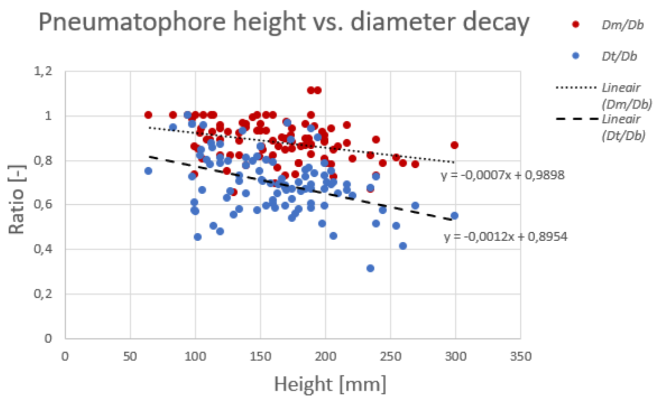

Figure 4.3: Pneumatophore height vs. diameter decay (All tree types combined)

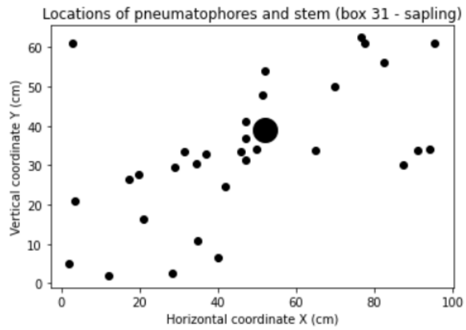

Figure 4.4: Root distribution of Box 31 (open sapling)

Pneumatophore locations

The locations of the pneumatophores for AV3111 (open sapling) have also been mapped and can be seen in Figure 4.4. The plot shows that the pneumatophores are not spread randomly over the box area, but they are in all likelihood connected to each other by underground roots. One can observe some patterns that radiate from the trunk towards the edges. Unfortunately, this underground root behaviour could not be investigated and it will (in nature) certainly be of influence for determining the locations of above-ground pneumatophores. However, in cases of a high root amount, roots will be spread practically everywhere around the trunk (within a certain zone). For these cases, the assumption of random locations might be viable. We will use this notion of randomizing root locations within our root model.

4.1.2. Canopy measurements

This section will highlight the results that were obtained after analysing all measured data of the branch structures for the four considered trees. Each branch order within a tree structure has its own properties. A more detailed description of each property is described in detail in Section 3.2.2. The measurement results are listed in Tables 4.2, 4.3, 4.4 and 4.5 for an open sapling, dense sapling, open (young) tree and dense (young) tree respectively. The open (young) tree consisted of multiple stems, however, we considered only the main stem results in Table 4.4. Lastly, branch diameters and -lengths for the dense tree were randomly measured (few measurements in view of time). However, we did register the full branching structure. Some things stand out when looking at the data, namely:

1. Dense trees contain more branches.
2. The average length of dense tree branches is generally lower than for open tree branches.
3. Diameter ratios vary significantly, however, most ratios fall in the range of 1.5-2.5 for a comparison between two subsequent orders: M and M_{-1}. Obviously, diameter ratios are higher for orders further apart.
4. Order [M,M_{-1},M_{-2}..] branch characteristics of saplings (Table 4.2, 4.3) are lower than for older trees (Table 4.4, 4.5)
5. Only the measured dense tree gives indication for L-system behaviour (see Section 3.7) since the average side branch amount for each branch is approximately equal (except for the main stem).

Table 4.2: Canopy measurements of a sparse sapling, approximately 1.5 years old.

branch order	quantity	μ_{Db} [mm]	σ_{Db} [mm]	μ_{Lb} [cm]	Db-ratio/O3	Db-ratio/O2	Db-ratio/O1	average side branch amount
4	1	15.04	-	101.40	2.78	3.71	3.76	11
3	6	5.58	0.94	54.40	-	1.6	2.48	2.67
2	16	3.70	0.65	39.57	-	-	1.66	2.31
1	42	2.43	0.52	23.48	-	-	-	-

Table 4.3: Canopy measurements of a dense sapling, approximately 1.5 years old.

branch order	quantity	μ_{Db} [mm]	σ_{Db} [mm]	μ_{Lb} [cm]	Db-ratio/O3	Db-ratio/O2	Db-ratio/O1	average side branch amount
4	1	19.47	-	79.39	2.61	-	-	5.00
3	5	7.59	1.08	57.39	-	2.15	2.78	8.80
2	26	3.61	0.80	37.93	-	-	1.93	4.15
1	126	2.24	0.49	17.30	-	-	-	-

Table 4.4: Canopy measurements of a sparse (young) tree, approximately 5 years old.

branch order	quantity	μ_{Db} [mm]	σ_{Db} [mm]	μ_{Lb} [cm]	Db-ratio/O4	Db-ratio/O3	Db-ratio/O2	Db-ratio/O1	average side branch amount
5	1	37.69	-	214.00	1.73	3.19	4.85	-	9.00
4	2	22.21	3.17	113.50	-	2.51	4.59	7.63	7.00
3	12	10.14	2.43	79.75	-	-	2.16	2.82	6.08
2	50	5.48	1.07	47.71	-	-	-	1.86	3.82
1	223	3.29	0.87	20.28	-	-	-	-	-

Table 4.5: Canopy measurements of a dense (young) tree, approximately 5 years old.

branch order	quantity	μ_{Db} [mm]	μ_{Lb} [cm]	Db-ratio/O5	Db-ratio/O4	Db-ratio/O3	Db-ratio/O2	Db-ratio/O1	average side branch amount
6	1	37.5	199.0	2.22	3.41	4.26	7.98	13.39	20.00
5	3	16.9	79.0	-	1.54	1.92	3.60	6.04	3.67
4	10	11	66.0	-	-	1.25	2.34	3.93	3.50
3	31	8.8	53.5	-	-	-	1.87	3.14	3.81
2	103	4.7	39.0	-	-	-	-	1.68	3.71
1	419	2.8	13.0	-	-	-	-	-	-

Branch diameter-length relationships

We established branch diameter-length relationships based on the measurements listed in Section 4.1.2. Average diameters and lengths of branch orders were plotted and the results are shown in Figure 4.5 for respectively sparse/open (blue) and dense (orange) *Avicennia m.* vegetation. Consequently, a (linear) trend line was fitted trough all the data points for both vegetation types. The equations give an approximation of branch length as function of branch diameter. In addition, a more general graph has been made that contains both vegetation types and field measurements data (Figure 4.6). Therefore, we made a crude assumption that the DBH of larger trees is approximately equal to it's highest order trunk mean diameter. This graphs serves as an order of magnitude estimator in the absence of canopy density information. All equations give reasonable estimates for very large branches that occur in nature. As a result, these relations were used to construct tree models for (very) old trees.

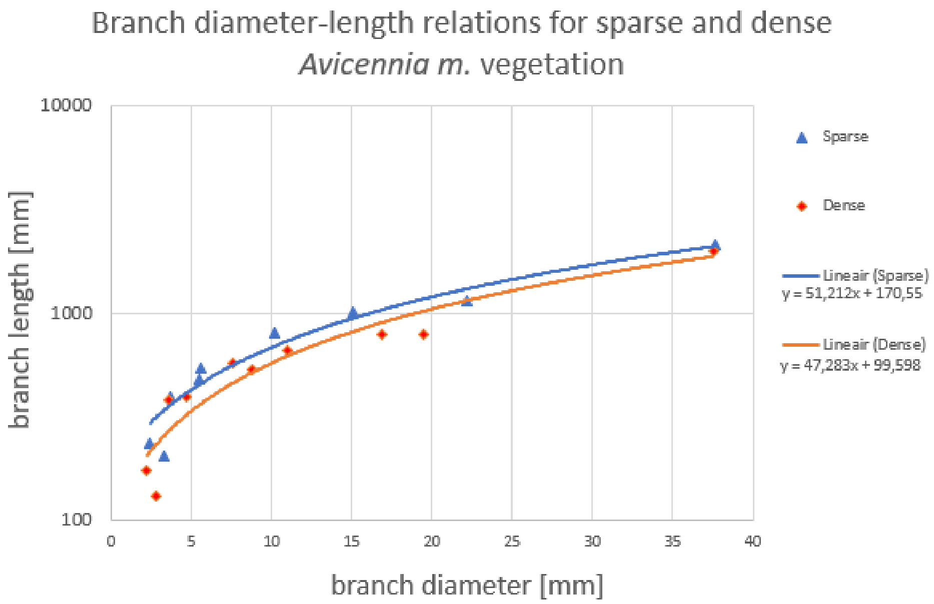

Figure 4.5: Branch diameter-length relationship for sparse and dense Avicennia marina vegetation

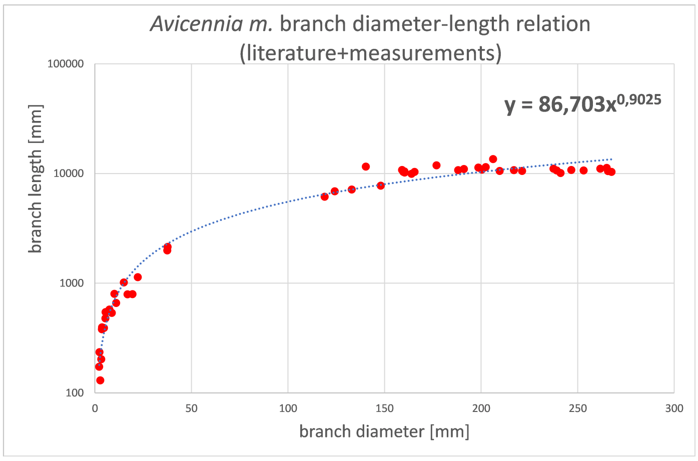

Figure 4.6: General branch diameter-length relationship (power function). This contains both field(Thailand) and greenhouse measurements.

Empirical (trend line) relations were found in Excel. The diameter-length relationships were established for each of the four tree types. However, we combined the results of the sapling and (young tree) for one type of vegetation density. A reasonable, linear fit was found and a distinction has been made between open (4.1) and dense (4.2 vegetation. One could could also establish a diameter-length relation based on all tree measurements (4.6) because in practice it is not always known beforehand if a tree canopy structure will turn out sparse or dense

$$L_b = 51.212D_b + 170,55 \tag{4.1}$$

$$L_b = 47.283D_b + 99.598 \tag{4.2}$$

with: branch length L_b [mm] and branch diameter D_b [mm]

4.2. Tree model results

The results of the 3D tree models can be found in this section. At first, we will treat the root model and canopy model separately. Thereafter, we combine both models to create complete tree models. The 3D models (meshes) can be exported by creating an stl-file. This is a particular file format that is often used for 3D models. It stores the data points in a specific manner such that it is easily recognizable by computer programs. The output data points from the models in Python are reworked by another function to store it as a STL-file.

4.2.1. Influence of the accuracy parameter for the designed geometrical models

Several model results are shown in this section. We start off with the results of one individual root with a varying value for nt. Figures 4.7 and 4.8 demonstrate the results for the situations with low accuracy (nt=6) and high accuracy ($nt = 100$) respectively. One can observe that for low nt value Figure 4.7 has an angular shape of the root circumference. This is not the case for nt being 100 (Figure 4.8) and one can see that the root shape is smooth and, therefore more realistic. Additionally, the high accuracy model contains more triangular faces and data points. However, the price for accuracy comes at the cost of computational power. Fortunately, the computation time is still short, even for root models that consist of more roots. Consequently, a higher value for nt is preferred. This fact also holds for other tree parts of the full tree model. It might be better to reduce nt for the construction of a set of trees / (small) forest model. Obviously, the selected value for nt does not affect the results for the frontal surface area computation.

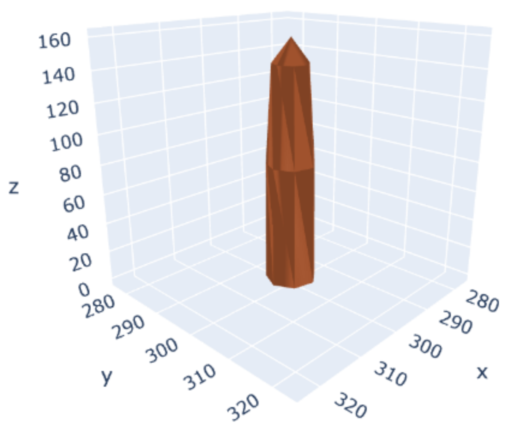

Figure 4.7: Root geometry for low nt value (nt=8)

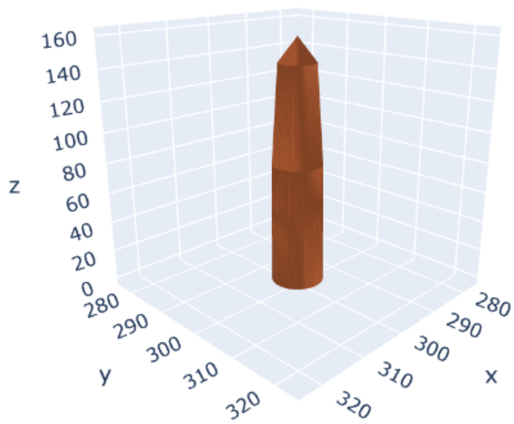

Figure 4.8: Root geometry for high nt value (nt=100)

4.2.2. Root model results

A configuration of pneumatophores is shown in Figure 4.9 and results from a model simulation of a young tree (5 years old) with a relatively low canopy density. However, the tree has four stems rising from the ground (from the tree buttress) which may cause a higher amount of root compared to single-stem trees. From Figure 4.9 follows that roots have a variable height and are randomly distributed over a fixed ground area. The fixed ground area is defined by the box dimensions that were measured in the greenhouse and equals 0.64 m^2. Obviously, the ground area that is occupied by roots of mature trees in nature is larger than this box area. Furthermore, one can observe from Figure 4.9 that roots will reach up to height of approximately 20 cm, which is in line with field measurements in former literature studies.

Figure 4.10 gives the root frontal surface area that is experienced by waves and currents when flowing through this dense array of roots (depicted in Figure 4.9). One can see that the frontal surface

area varies significantly over the height. A decaying frontal surface area is observed which must be the case since less roots contribute to the frontal surface area at larger heights. Additionally, the root diameter decay over the height results in a enhanced decline in root frontal surface area. A step plot has been generated that accounts for vertical layers thickness (vlt) equal to 1 mm. Practically all roots are present in the 0 to 10 cm range and diameter decay is small for the base-middle reach of the roots. This can also be observed from the frontal surface area plot. At heights larger than 10 cm, the total frontal surface area decreases rapidly which is in line with our expectations. One can see that absence of roots at heights larger than 20-25 cm can also be derived from Figure 4.10.
The root model of Figure 4.9 can be exported from the coding environment by rewriting the model data points into STL-file format. Consequently, one arrives at the model depicted in Figure 4.11. This STL-file root model can be further investigated with practically all 3D software programs.

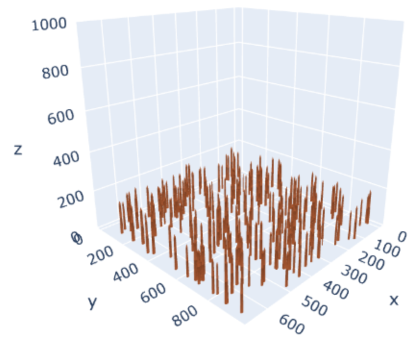

Figure 4.9: Root model for a (young) tree (5 years old) with low canopy density. The model contains 246 roots in total.

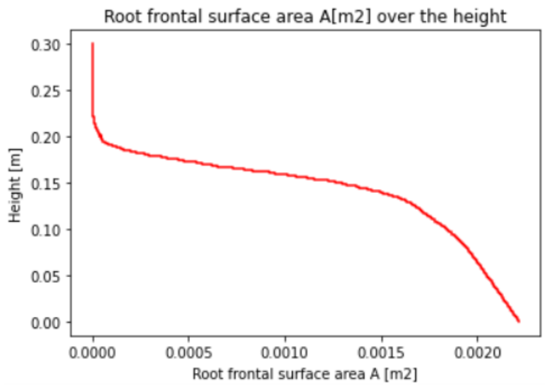

Figure 4.10: Frontal surface area distribution of a root model (5 year old open tree). The displayed root frontal surface area on the x-axis is expressed for layers of 1mm over the total height

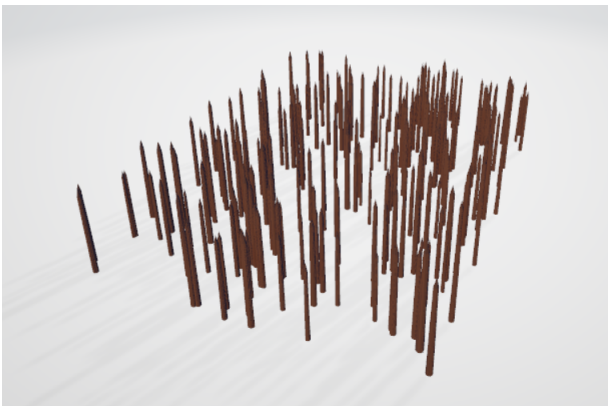

Figure 4.11: Exportable STL-file of 3D root model from Figure 4.9

To highlight the differences in root models for different tree ages, we included also the model results of a sapling (2 years old) with comparable canopy density (sparse/open) as the above-mentioned root model results. The root model results and root frontal surface area distribution over the height (over layers of 1mm) are shown in Figures 4.12 and 4.13 respectively. What immediately stands out is the reduced amount of roots and frontal surface area. Moreover, the roots appear to be slightly smaller compared to the model for a five-year old specimen. The latter is mainly due to a lower standard deviation of root diameters for a young sapling, resulting in fewer outliers of branch lengths. Lastly, one can observe that the first two to three layers have the largest share of root frontal surface area (similar as the case for an open tree). The governing water level determines at what above-ground height wave-vegetation interaction will occur and, consequently the rate of dissipation by roots. Fully submerged roots are less effective in attenuating waves but more effective in attenuating currents.

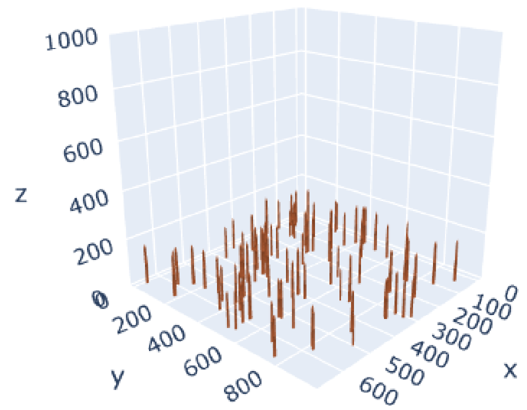

Figure 4.12: Root model for a sapling (2 years old) with low canopy density.

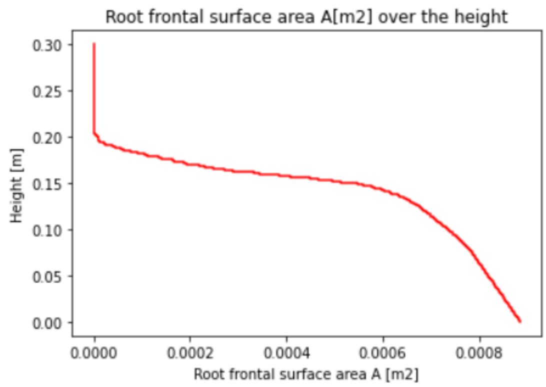

Figure 4.13: Root frontal surface area distribution over the height for a sapling (2 years old) with low canopy density

4.2.3. Canopy model results

Canopy model 1

Canopy model 1 constructs the canopy geometry as mentioned in Section 3.5.1. To summarize, the diameters of the branches are dependent and determined by diameter ratios between subsequent branch orders. The advantage of this model is that one could provide one single input value, namely the tree trunk diameter and, based on that, compute the whole system of branches through dependency relations. The downside of this methodology is that the fixed diameter ratios between different orders will result in similar branch diameters for each order. Consequently, the tree model shows less variability in branch dimensions within a certain branch order class than canopy model 2, which is explained later. Four different tree types were generated and are shown in Figures 4.14,4.16, 4.18 and 4.20, together with their respective frontal surface area distributions (Figures 4.15,4.17,4.19 and 4.21).

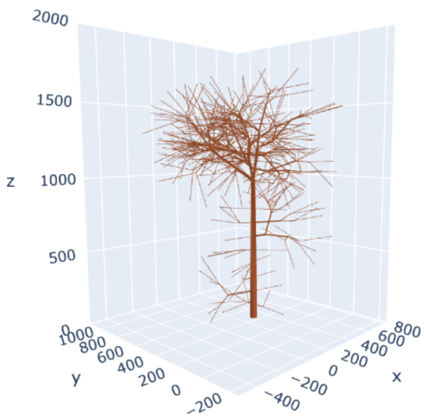

Figure 4.14: Canopy model for a young, dense tree (5 years old)

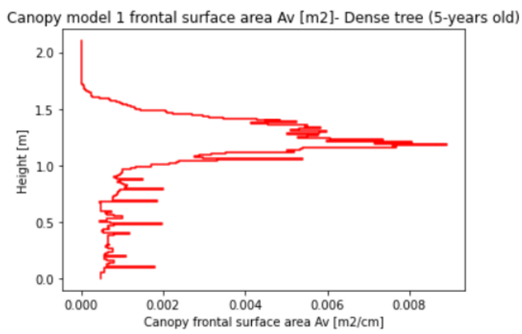

Figure 4.15: Canopy frontal surface area distribution over height for a young tree (5 years old) with high canopy density. Chosen layer thickness was 1cm.

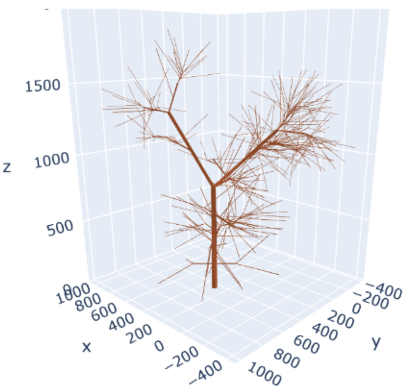

Figure 4.16: Canopy model for a young, dense tree (5 years old)

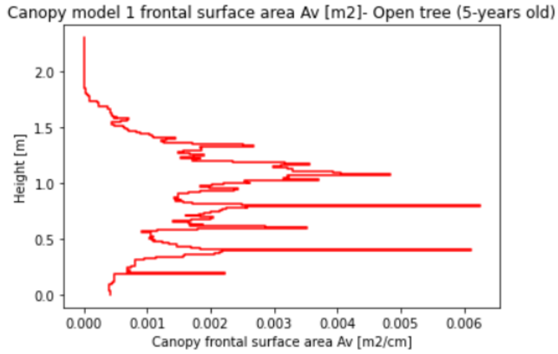

Figure 4.17: Canopy frontal surface area distribution over height for a young tree (5 years old) with high canopy density. Chosen layer thickness was 1cm. Total Av = 0.27 m2.

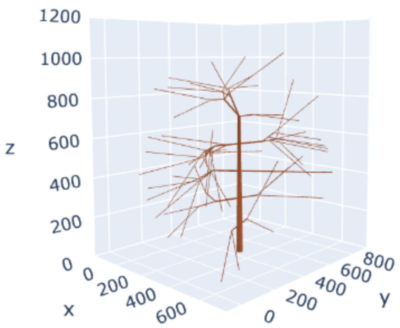

Figure 4.18: Canopy model for an open sapling (2 years old)

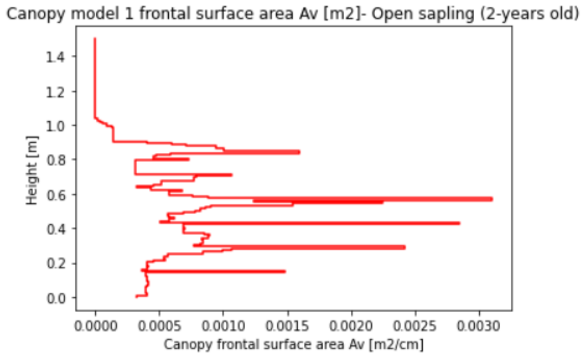

Figure 4.19: Canopy frontal surface area distribution over height for a young tree (5 years old) with high canopy density. Chosen layer thickness was 1cm. Total Av = 0.07 m2.

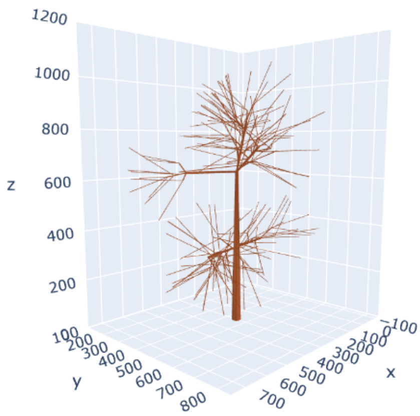

Figure 4.20: Canopy model 1 for a dense sapling (2 years old)

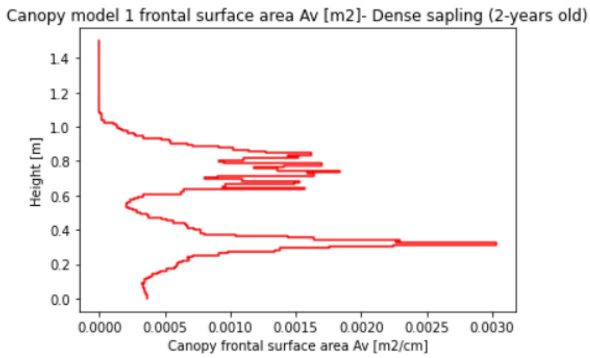

Figure 4.21: Canopy model 1 frontal surface area distribution over height for a dense sapling (2 years old). Chosen layer thickness was 1cm. Total Av = 0.08 m2.

Canopy model 2

For canopy model 2, branch diameters have been determined by the normal distribution of branch diameters for each branch order. Parameters for normal distributions are estimated based on the tree measurements from the greenhouse. The normal distribution parameters are extrapolated or interpolated depending on the desired tree age. Models have been generated for all tree types, varying in age and density. Again, a vertical layer thickness of 1cm (vlt=10) was chosen to obtain a quasi-continuous frontal surface area distribution. The frontal surface area Av is shown in m2 for a layer with thickness 1cm at a given height of the tree.

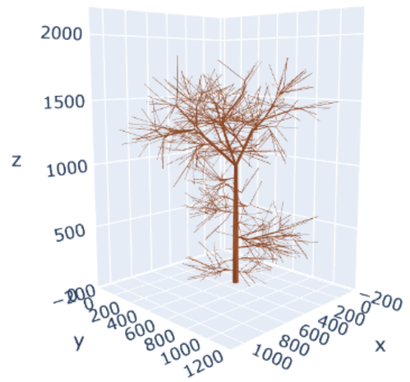

Figure 4.22: Canopy model for a young, dense tree (5 years old)

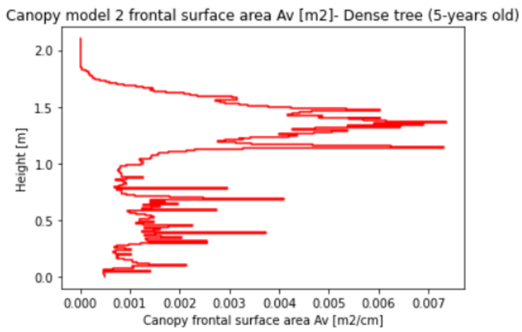

Figure 4.23: Canopy model 2 - frontal surface area distribution over the height for a young, dense tree (5 years old) over layers with 1cm thickness.

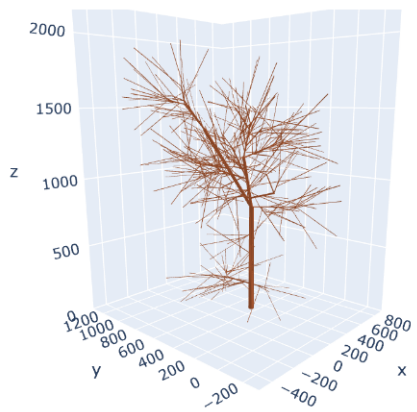

Figure 4.24: Canopy model for a young, sparse tree (5 years old)

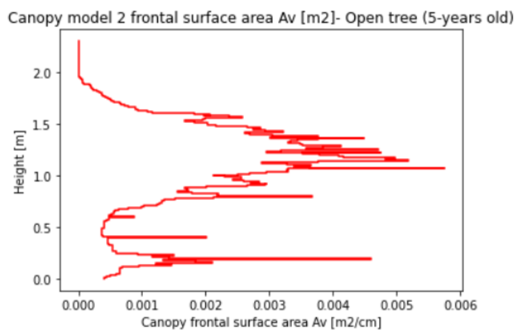

Figure 4.25: Canopy model 2 - frontal surface area distribution over the height for a young tree (5 years old) with high canopy density over layers with 1cm thickness. Total Av = 0.32 m2.

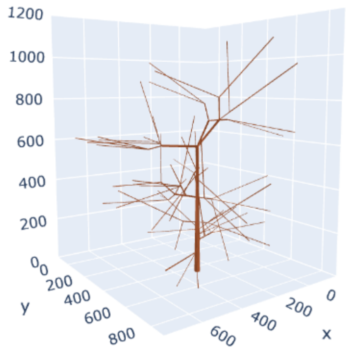

Figure 4.26: Canopy model for a young, dense tree (5 years old)

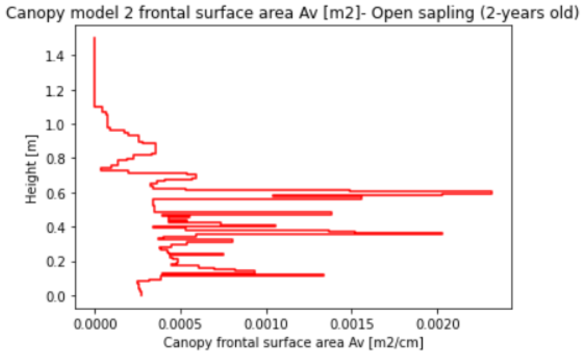

Figure 4.27: Canopy frontal surface area distribution over height for a young tree (5 years old) with high canopy density. Chosen layer thickness was 1cm. Total Av = 0.05 m2.

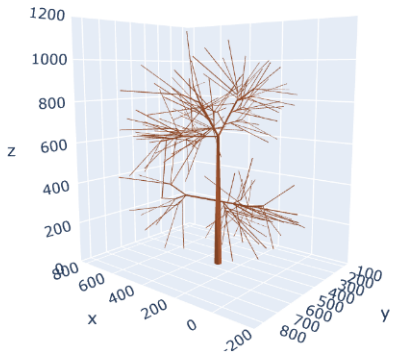

Figure 4.28: Canopy model for a dense sapling (2 years old)

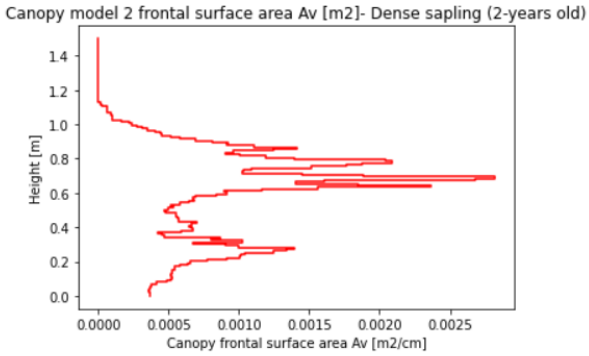

Figure 4.29: Canopy frontal surface area distribution over height for a dense sapling (2 years old). Chosen layer thickness was 1cm. Total Av = 0.09 m2.

4.2.4. Range of Av(z) results for all tree types

The frontal surface area distribution over the height (AV) mainly depends on the orientation-, number- and type of branches. These aspects are determined by the tree models in a random or probabilistic manner. Therefore, we simulated 100 trees for all tree types and each canopy model and, as a result, ranges/bandwidths are obtained that shows the average frontal surface area distribution and the 95% confidence interval. The frontal surface area contribution of the roots has also been included in the results.

Open sapling

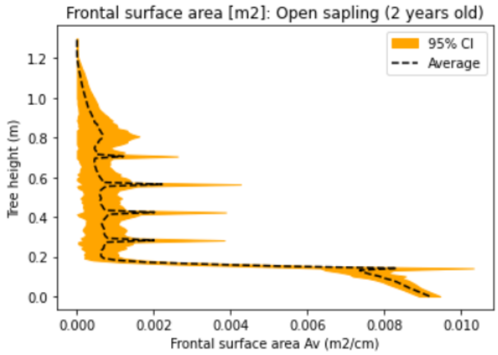

Figure 4.30: 95% confidence interval of Av distribution for an open sapling (2 years old) with canopy model 1, including roots.

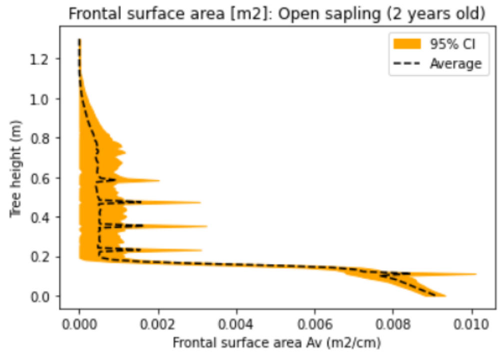

Figure 4.31: 95% confidence interval of Av distribution for an open sapling (2 years old) with canopy model 2, including roots.

Table 4.6: Total frontal surface area 95% bandwidth (m2) for tree type: open sapling (2 years old)

model	lower limit Av [m2]	average Av [m2]	upper limit Av [m2]
model 1	0.13	0.19	0.25
model 2	0.12	0.17	0.22

Dense sapling

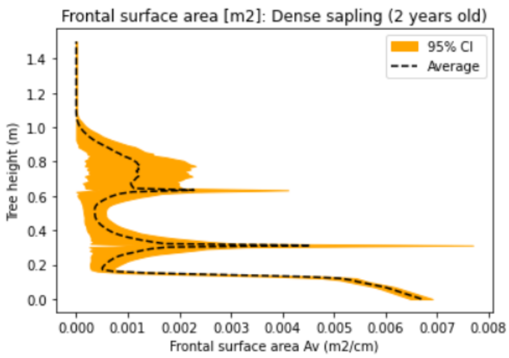

Figure 4.32: 95% confidence interval of Av(z) for a dense sapling (2 years old) with canopy model 1, including roots.

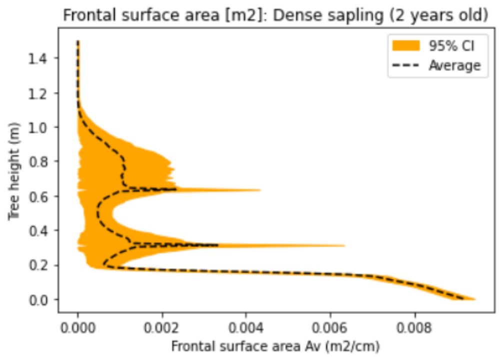

Figure 4.33: 95% confidence interval of Av(z) for a dense sapling (2 years old) with canopy model 2, including roots.

Table 4.7: Total frontal surface area 95% bandwidth (m2) for tree type: open sapling (2 years old)

model	lower limit Av [m2]	average Av [m2]	upper limit Av [m2]
model 1	0.1	0.16	0.22
model 2	0.13	0.20	0.27

Dense tree

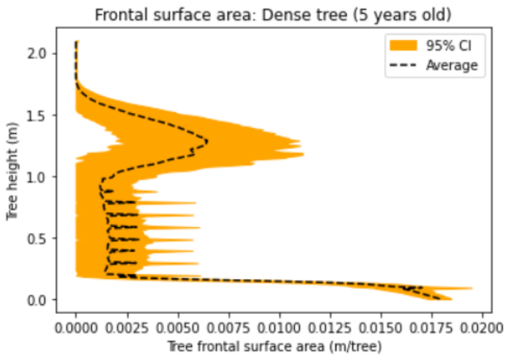

Figure 4.34: 95% confidence interval of Av(z) for a dense sapling (2 years old) with canopy model 1, including roots.

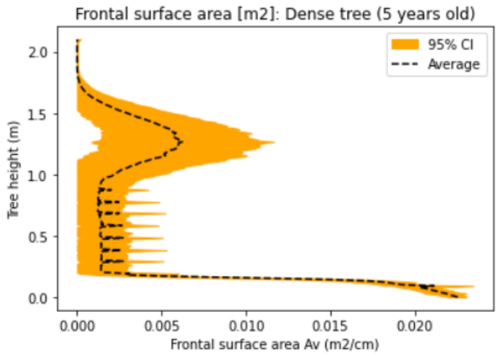

Figure 4.35: 95% confidence interval of Av(z) for a dense tree (5 years old) with canopy model 2, including roots.

Table 4.8: Total frontal surface area 95% bandwidth (m2) for tree type: open sapling (2 years old)

model	lower limit Av [m2]	average Av [m2]	upper limit Av [m2]
model 1	0.28	0.65	1.04
model 2	0.35	0.72	1.11

Open tree

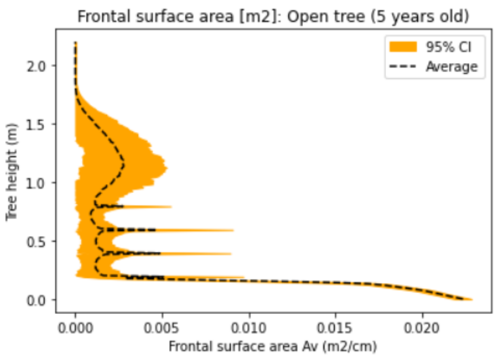

Figure 4.36: 95% confidence interval of Av(z) for an open tree (5 years old) with canopy model 1, including roots.

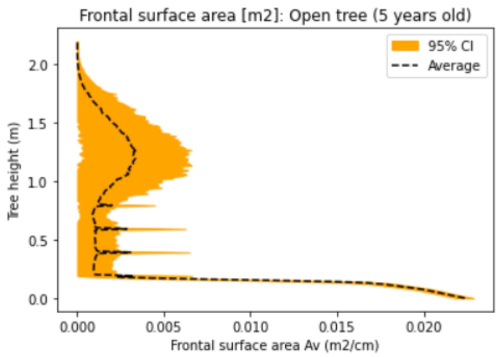

Figure 4.37: 95% confidence interval of Av(z) for an open tree (5 years old) with canopy model 2, including roots.

Table 4.9: Canopy models 1 and 2: $Av(z)$ 95% bandwidth (m2) for tree type: open tree (5 years old)

model	lower limit Av [m2]	average Av [m2]	upper limit Av [m2]
model 1	0.33	0.57	0.81
model 2	0.31	0.60	0.93

4.2.5. Tree model generation for various tree ages through extrapolation and interpolation of data

Due to limited tree measurements, it is necessary to interpolate and extrapolate data to obtain estimates of frontal surface area distributions for tree ages other than 1.5 years and 5/6 years. The measurements of a 1.5 year old sapling and a 5/6 year old tree allow us to interpolate data for tree ages in between this range. As mentioned before, canopy models 1 and 2 are fundamentally different in defining the canopy geometry. Therefore, we elaborate on this in two separate sections.

Canopy model 1

Canopy model 1 is the deterministic way of finding branch geometries. The only parameter that we must know is the initial stem diameter. All other branch dimensions follow from this initial value. Consequently, empirical relations are found to relate tree age to tree stem diameter. For tree ages > 1.5 y and < 6 y, measurement data was interpolated. For tree ages > 6 y, an allometric relation is applied to determine the stem diameter (see Figure 2.3a). It follows that:

$$D_{stem}(X_{age}) = \begin{cases} -1.1381X_{age}^2 + 13.21X_{age}, & \text{if } 1.5 <= X_{age} < 6 \\ 10.8X_{age} - 26, & \text{if} X_{age} >= 6 \end{cases}$$

We found that for a tree age of 6 years, D_{stem} is equal at the transition of the conditional statements. A simulation of 20 year old tree model without roots is shown in Figure 4.38.

Canopy model 2

Canopy model 2 is probabilistic and, therefore, it is important to distinguish between various branch orders since branch dimensions are no longer dependent on each other. Consequently, we take into account all branch orders and not only the stem diameter. The data analysis that followed from the greenhouse measurements resulted in normal distribution parameters (μ_{Db} and σ_{Db}) for each branch order for tree ages 1.5 and 5 years (see Section 4.1.2). These parameters are being extrapolated for tree ages larger than 5 and interpolated in all other cases. The model then computes branch dimensions based on the newly defined normal distribution. The outcome of a CM2 simulation is shown in Figure 4.39.

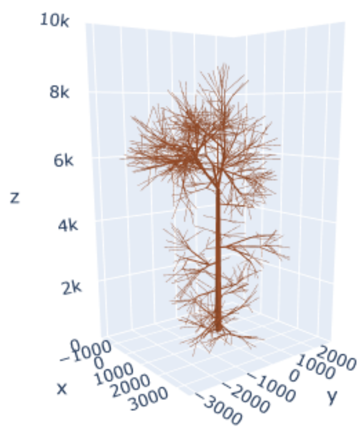

Figure 4.38: 20 year old tree (simulation of canopy model 1)

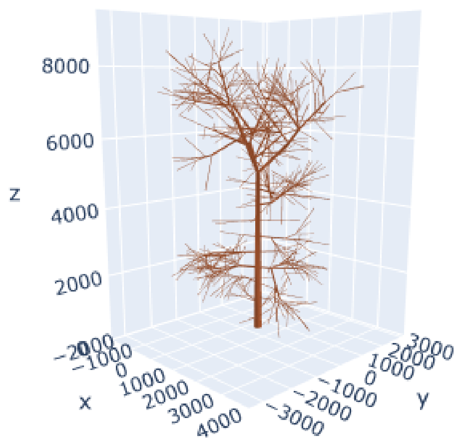

Figure 4.39: 20 year old tree (simulation of canopy model 2)

The simulated results of CM1 and CM2 for 20-year old trees correspond well with the measured data set from Intarat and Vaiphasa (2020) that can be found in Table A.2 and consist only of mature trees.

4.2.6. Oblique tree stems

Tree stems are often not completely straight and often grow under an angle. Figure 4.40 illustrates a tree model with a stem growing at an oblique angle. Changing the angle of the stem influences the positioning of other branches as can be seen in Figure 4.40. Random angles can be assigned (within a realistic range) to stems of multi-stemmed trees.

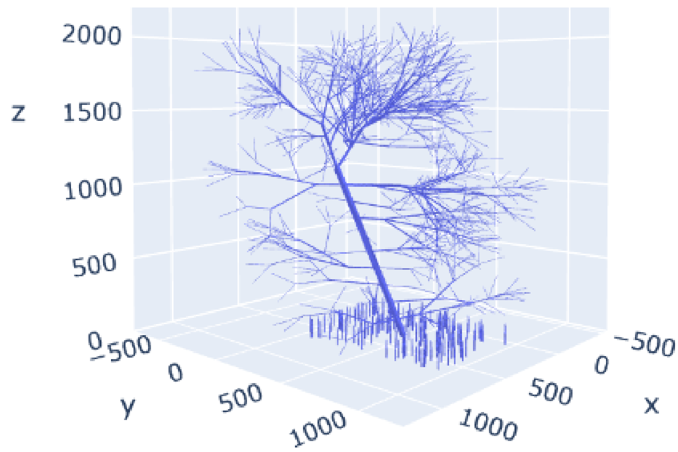

Figure 4.40: A tree model with a stem growing at an oblique angle.

4.2.7. Multi-stemmed trees

The generation of multi-stemmed tree models is realized by fixing the starting position of all stems and to provide a viable, random orientation to each of the stems, which defines the direction of growth. The difficulty is predicting when a tree will contain multiple stems and, if so, how many stems. Besides, each stem may have a different diameter/order. This requires more observations and measurements to come up with appropriate estimations regarding multi-stemmed tree geometry.

4.2.8. Share of different branch classes to total frontal surface area

Simulations for older trees demonstrate that the contribution of smaller order branches to the total projected frontal surface area Av is significantly large. An example is shown in Figure 4.41 with the distribution of Av per branch order class shown in Table 4.10. The tree stem is indicated with order 6 and the smallest twigs are indicated with order 1.

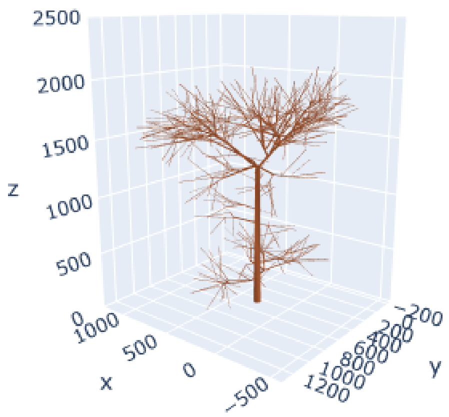

Figure 4.41: Tree model (six years old)

Table 4.10: Distribution of Av (0.4868 m2) over all branch order classes

branch order	6	5	4	3	2	1
Av [m2]	0.05	0.02	0.005	0.08	0.09	0.238
% share	10	4	1	17	19	49

Therefore, the summation of Av's due to all smaller order branches is larger than for the largest order branches. This emphasizes the importance of taken into account smaller branches as they contribute largely to the total frontal surface area of the tree.

4.2.9. Model validation

For tree model validation, greenhouse trees were divided in seven vertical layers over the tree height. The size of the layers depended on the tree height. For an arbitrary layer, branch orders were registered that intersected with the layer. The frontal surface area of a branch order was determined by the product of the average length and average diameter for that order. Consequently, The frontal surface area of a layer was defined as the summation of all branches. The set-up is shown in Figures 4.42 and 4.43 for an open sapling and open tree respectively. Layer transitions were indicated with red tape. Validation measurements were also performed for a dense tree. This validation method was too difficult to be applied for a dense sapling because of it's high branch density, twisting branches and complex structure in general. The applied validation method generally yields an upper limit for the projected frontal surface area because branch orientations are neglected. It is expected that this leads to an overestimation of the frontal surface area over the height. A model validation by image analysis was also considered but it was concluded that this was difficult to execute due to the limited space in the greenhouse, close proximity of other trees and blockage by leaves. It was for this reason that we continued with registering the number of branches per layer as a validation method for the developed tree models.

Figure 4.42: Open sapling model validation set up with 7 vertical layers of 20 cm

Figure 4.43: Open tree model validation set up with 7 vertical layers of 40 cm

The estimated frontal surface areas that resulted from the validation measurements were then compared to the output results of the various tree models. Both the frontal surface area results of canopy model 1 and canopy model 2 were evaluated for an open sapling (Figures 4.44, 4.45, open tree (Figures 4.46, 4.47 and dense tree (Figures 4.48, 4.49. For each tree type, 100 simulations were performed to obtain the average $Av(z)$ and the upper limit of the 95% confidence interval of $Av(z)$ (for 7 vertical layers).

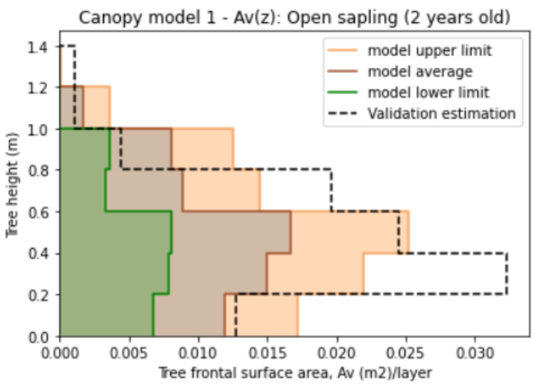

Figure 4.44: Av(z): Canopy model 1 vs. validation measurements

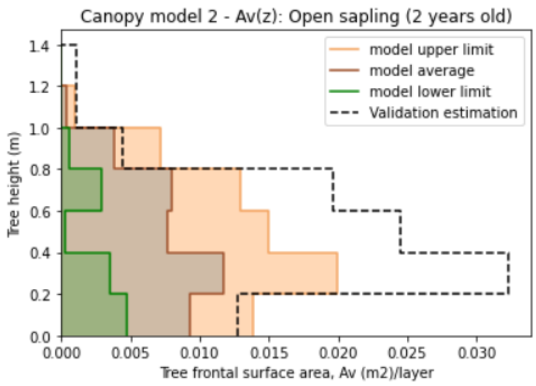

Figure 4.45: Av(z): Canopy model 2 vs. validation measurements

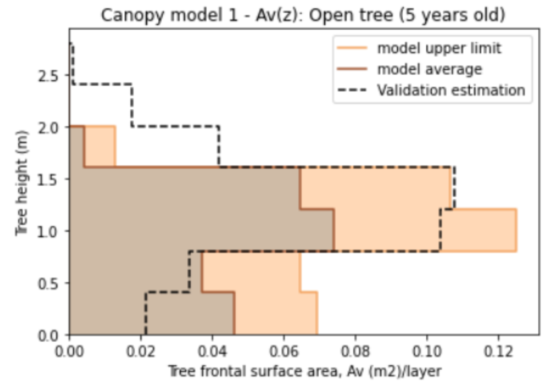

Figure 4.46: Open sapling model validation set up with 7 vertical layers of 20 cm

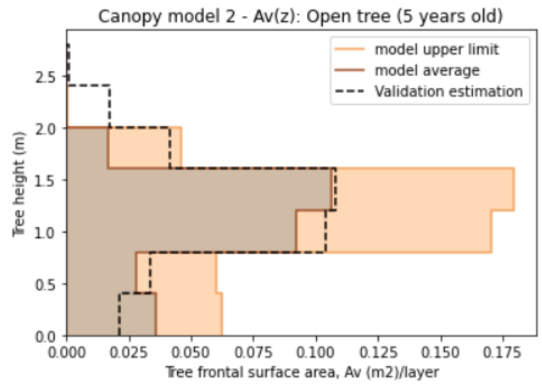

Figure 4.47: Open tree model validation set up with 7 vertical layers of 40 cm

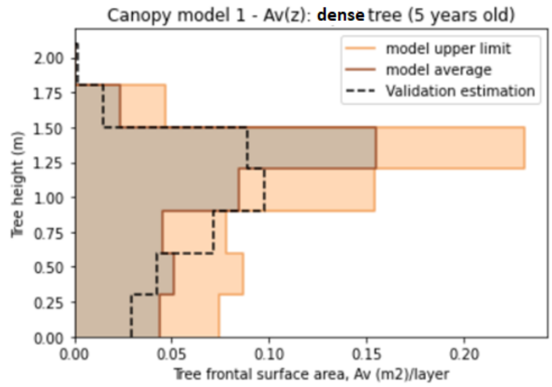

Figure 4.48: Av(z): Canopy model 1 vs. validation measurements

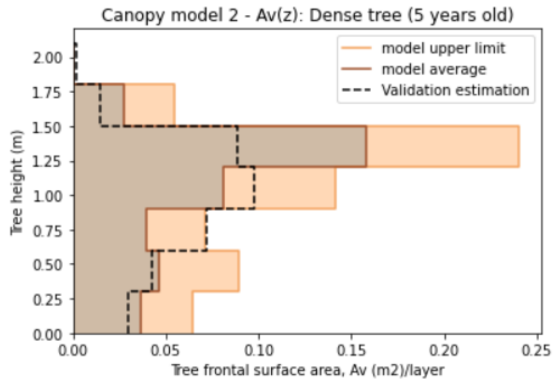

Figure 4.49: Av(z): Canopy model 2 vs. validation measurements

Based on the results, it is concluded that for a 2-year old sapling with low canopy density, canopy model 1 approached the total frontal surface area slightly better. However, the distributions of frontal areas over the height show better similarities with canopy model 2. It was observed that the tree had grown strongly over the past few months which could have resulted in differences between the validation and canopy models in terms of total projected frontal area. Although, the tree models account for growth, the tree growth might have turned out larger than predicted.

For the 'open tree' model validation, canopy model 2 showed better agreement with the validation measurements. It can be observed that both in the high vegetation layers and in the lower vegetation layers, projected frontal areas are better approximated by canopy model 2. The highest vegetation layer (2m-2.5m) is not well covered by both canopy models, which indicates that the developed tree models are slightly shorter than the real trees.

At last, a validation analysis was done for 'dense tree' models. In general, both canopy models cover projected frontal surface areas relatively well and there is no clear indication that one canopy model performs better. However, the vegetation layer higher up in the canopy (1.25m-1.50m) showed a mismatch between the model results and validation measurements. It is unclear what causes this mismatch, as this could have multiple causes. A new validation for an arbitrary dense tree could provide more insights into the validity of the developed tree model.

5 Discussion

Recent studies by Kalloe et al., 2022 and van Wesenbeeck et al., 2022 highlighted that the projected frontal surface area of woody vegetation is a crucial parameter for wave attenuation. The goal of this study was to generate geometrical tree models of *Avicennia marina* vegetation to determine the frontal surface area distribution over the vertical coordinate $Av(z)$ and, by doing this, provide potential tools for estimating wave attenuation my mangrove vegetation. In other words, this study was meant to offer another perspective in quantifying the effectiveness of nature-based solutions regarding wave attenuation. In order to achieve this, we aimed to capture the full tree geometry of *Avicennia marina* vegetation that consists of the tree stem, canopy and roots for a wide range of tree growth stages and canopy density characteristics.

According to the current state of affairs in literature, several approaches exist to describe wave damping by vegetation. Vegetation could be schematized as uniform cylinders (Dalrymple et al., 1984) or more refined, as cylinders with representative diameters over multiple vegetation layers (Suzuki, 2011). Maza, Lara, et al. (2021) modelled wave attenuation by mangrove vegetation as function of submerged vegetation volume. Lastly, several studies describe wave attenuation as function of vegetation frontal surface area (Mazda et al., 1997; van Wesenbeeck et al., 2022; Kalloe et al., 2022). The frontal surface area distribution over the height provides important information of the vegetation characteristics over the full height of the water column. Moreover, most other parameters can easily be deduced from a frontal surface area distribution $Av(z)$. Therefore, an effort was made to refine current (simplistic) mangrove models by the development of geometrical mangrove models with associated $Av(z)$ by accounting for variations in vegetation area over the vertical coordinate.

An important note is that the model considers the same amount of branch orders as the situation for a 5 year old tree. However, it is more likely that a wider range of branch orders will be present for the 20 year old tree. Consequently, the current model underestimates the total frontal surface area of old trees. More measurements are needed to map the distribution of branch classes as function of age. One can also assume, based on the measurements, that the smallest order branches have a diameter of 3/4 mm. Consequently, one can estimate when an additional branch order class is added to the tree system based on previous branch ratios.

5.1. Model limitations

Limitations in time have led to a limited amount of measured data that was used for the construction of the tree models. Only four trees were measured, one of each tree type and, more data was extracted from this by interpolation and extrapolation of the data. This limited amount of data imposes limitations on the developed tree models. Measuring more trees of similar tree types can confirm or contradict established relations which is valuable information for the design of the tree models. The addition of more data will positively influence the model reliability by excluding uncertainties. The most important relations worth checking are:

- root quantity as function of tree age/above-ground biomass (roots contribute significantly to the frontal surface area in the lower vegetation layers so this must be accurately defined)
- branch length as function of branch diameter for all branch orders and tree types
- amount of different branch orders as function of tree age/density
- angles of side branches with respect to the main branch
- tapering of branches
- information regarding stem quantities and growing angles for various tree types

If these points are correctly defined within the model, then the tree model is likely to improve considerably.

The trees that were measured can be classified as artificial because they grow in a controlled "greenhouse" environment with limited space and possibly other limitations compared to natural, mangrove trees in (sub)tropical regions. Since we only measured the trees in the greenhouse, some uncertainty . The question is whether the measured/observed tree characteristics are relatable to the tree characteristics of natural trees. This should be checked. However, the tree models are able to reach heights up to 10-11 m for high age values. This is in line with results from literature from which was found that mature trees are approximately this height (Intarat & Vaiphasa, 2020).

An important note is that the tree models for high ages (15-20 years) consider the same amount of branch orders as the situation for a 5 year old tree. However, it is more likely that a wider range of branch orders will be present for the 20 year old tree. Consequently, the current model underestimates the total frontal surface area of old trees, which is a model limitation. More measurements are needed to map the distribution of branch classes as function of age. One can also assume, based on the measurements, that the smallest order branches have a diameter of 3/4 mm. Consequently, one can estimate when an additional branch order class is added to the tree system based on previous branch ratios.

The presence of leaves were neglected in the development of the tree model under the assumption that these contribute little to the frontal surface area. This conclusion has been made based on a study by van Wesenbeeck et al. (2022). However, this study focused on willow trees so it is useful to check if this also hold for mangroves. Branch tapering has only been applied to the tree stems because this information followed clearly from diameter measurements over the stem length. For smaller order branches, relations were often not unambiguous. It is worthwhile to further investigate branch tapering and insert this information into the tree model backbone in order to come up with a more refined model. Another limitation of the current tree model is that vegetation flexibility is not yet taken into account.

A way to consider flexibility is to measure the force required to deflect a certain branch order and compare that to the applied wave forces. As a result, estimations can be made on the reduction of frontal surface area over the height due to flexibility. For example, smaller branches are more likely to deform and position themselves in a more streamlined orientation, causing a reduction in frontal surface area. However, the tree stem is often more rigid and generally less sensitive to wave forces.

Lastly, this study only considered individual trees (small-scale) yet and not a strip or forest with multiple trees, although this is relatively easy to implement because essentially it is just a collection of individual tree models within a certain predefined forest area.

5.2. Interpretation of the results

This study succeeded in the construction of geometrical tree values from which the frontal surface area distribution could be obtained. Each branch contained data of their location in 3D space and with this information, we could deduce the projected frontal surface area for a given direction of interest. First, root measurements were performed and modelled. It was found that root measurements (base diameter and root height) are in agreement with former pneumatophore studies (Jordan and Frohle, 2022; Jusoh et al., 2016; Thampanya, 2006). We established normal distributions for root base diameters based on 25 measurements/tree type (100 measurements in total). It followed that the root model provides realistic geometries of roots, in line with literature and observations. A critical note is that the variability in root heights resulting from the model is less than the actual situation. This is probably due to the linearized relation that was found between root base diameter and root height. Observations in the greenhouse showed that not in all cases, an increase in root base diameter will automatically lead to a higher root height. Our implemented linear relation between root base diameter and root height causes the roots to be less variable and, as a consequence, not often exceeds 20 cm in height.

As a follow-up, canopy measurements were performed to obtain data on branch diameters, -lengths and -distributions of orders for various tree types. With this information, two canopy models were created:

1. **canopy model 1**: estimates branch diameters of newly generated branches based on ratios with preceding branches (more deterministic approach). An advantage of this model is that only one initial value, namely the stem diameter is needed to generate the full canopy geometry. The downside is less variability between branch geometries of the same class.
2. **canopy model 2**: estimates branch diameters based on measured normal distribution parameters for respective branch orders (more probabilistic approach). An advantage of this model is that it accounts for variability in branch dimensions within a certain branch class and, thus mimics natural variability. The downside is the need for normal distributions that have to be set up based on many tree measurements.

A hundred simulations were performed for each tree type (root model and canopy model combined) to obtain the 95% confidence interval (bandwidth) of the projected frontal surface area distribution $A(v)$ over the tree height for a given direction. From this followed that $Av(z)$ in the lower layers was highest and dominated by the presence of roots. Therefore, it is important to always account for roots in modeling efforts. Furthermore, the canopies, often starting at approximately half the tree height, also lead to a significant increase in frontal surface area and must therefore also been taken into account for high water levels. The importance of $Av(z)$ due to roots and canopies increases for increasing tree age and canopy density. The effect of smaller order branches to the total frontal surface area is therefore very significant.

We found that the output results of $Av(z)$ from canopy model 2 and canopy model 1 are fairly similar. Based on the chosen validation method, no clear conclusions are drawn on which model performs better and which model can be excluded. It appeared that the validation method itself was an overestimation of the total frontal surface area which led to discrepancy in results between the validation measurements and the tree models. We saw from the validation measurements that that the top two layers were often less well described by the model. Thus, the tree models should be improved to match this small difference in tree height. The way to improve this is to perform additional measurements and establish (potentially) new branch diameter-length relations that result in larger branch lengths. Alternatively, the branching angles may be adjusted to cause branches to grow in a more upward/vertical direction instead of horizontally. It can also be argued whether the selected tree ordering system is suited enough to describe and generate tree geometry of $Avicenniam$ vegetation. For now, it does seem like an appropriate choice.

5.3. Implications for future research

The results of this study show that it is indeed important to account for the full frontal surface area distribution $A(v)$ as this parameter considers all vertical vegetation layers. It is concluded that pneumatophores (roots) play a major role in the first 0m-0.3m above ground level. The canopy is also a major contributor to the frontal surface area and starts often halfway the height of *Avicennia m.* vegetation. Therefore, the considered vegetation is not well represented by the stem only and this should be accounted for in further modeling practices.

The generated tree models might open up new ways of thinking with respect to geometrical vegetation modeling for hydrodynamic analysis. The study showed that it is possible to construct geometrical models based on measured data and to provide improved estimations of total frontal surface area with respect to current cylinder representations. Improvements could be made to the tree models based on laser scanned data and/or additional hand measurements. The study offers an alternative view on estimating frontal surface areas without relying on laser-scanning/imaging techniques.

6 Conclusions

The goal of this study was to provide estimates of the frontal surface area distribution of *Avicennia marina* vegetation by generating geometrical tree models for a range of tree sizes/ages. Based on the results, we conclude that it is possible to construct a geometrical tree model of *Avicennia m. vegetation* as function of age (for a wide range of ages) that provides practical information of the frontal surface area distribution over the vertical coordinate, $Av(z)$. This $Av(z)$ can then be used as parameter for modelling wave-vegetation interaction. Geometrical tree models consist of an integrated root model and canopy model (including stem).

6.1. Root measurements and root model construction

The root model was constructed based on measurements that were performed on trees (in the greenhouse) with various characteristics. Probabilistic distributions of root diameters were obtained that were linked with the root length and, consequently, root shape. With these known parameters, data points were created to define the geometrical model and $Av(z)$. It was found that larger roots have a more conical shape, while smaller roots are more cylindrical. Furthermore, root height measurements corresponded well with former literature studies. It still remains uncertain how the distribution of roots around a tree changes for tree ages larger than 5/6 years.

6.2. Canopy measurements and canopy model construction

First, canopy measurements were performed for an open sapling (1.5 years old), dense sapling (1.5 years old), open tree (5 years old) and dense tree (5 years old) and the data was analysed. Differences in branching systems were observed between open and dense vegetation. Dense vegetation consisted of more branch order classes compared to open vegetation. Differences were also observed between various tree ages regarding branch order classes and diameters. For canopy/tree model 1, we only estimate the stem diameter based on measured, empirical relations (for trees < 6 years) and allometric relations from literature (for trees > 6 years). For canopy/tree model 2, probabilistic data is extrapolated for mature trees (> 6 years) and interpolated for tree ages between 1.5 years and 6 years in order to compute branch dimensions as function of tree age. From all this followed important branching relations and structural parameters that were used as a blueprint for the tree models.

Two different canopy models were constructed that each build upon a different principle. Canopy model 1 (deterministic) takes dependent branch relations into account to determine the branch diameter, Db, of a new branch. Canopy model 2 (probabilistic) determines Db based on the normal distribution of branch diameter measurements for each branch class. Canopy model 1 shows more similarities to a L-system (see Section 2.1.4) because of its deterministic, repetitive nature and, therefore, is better applicable in computational models due to its ease of use and efficiency. By analysing the measured branch data, branch length could be related to the branch diameter and, consequently, the branch geometry could be determined. The branches were correctly placed within the canopy system by a programmed algorithm.

6.3. Tree model results

A hundred simulations for each tree type were performed (full tree model: roots+canopy) to obtain a 95% confidence interval range of possible $Av(z)$. Also the average values were shown. It was found that the roots contributed most to the the frontal surface area distribution of *Avicennia m.* vegetation, although this only applies for the first three decimeters above ground level. Canopies were also a major contributor to $Av(z)$. Both roots and canopy should therefore always be included in modeling wave attenuation by *Avicennia m.* vegetation. We found that smaller order branches contribute significantly to $Av(z)$ for larger/older trees and, for the simulated tree models, showed a higher $Av(z)$ than the higher order branches (such as the stem).

Tree models were validated by performing validation measurements. An open sapling (2 years), open tree (5 years) and dense tree (5 years) where divided into seven distinct vertical layers and branches were counted that intersected with each layer. Thereafter, based on the branch count, estimations were made regarding the frontal surface area for each layer. The results were later compared to the tree model outcomes. It followed both canopy models showed little differences. Therefore, the results are inconclusive. Another validation method is recommended. We found that canopy model 1 is more practical due to its ease of use. Little information is necessary in order to create a geometrical tree model which favours canopy model 1 over canopy model 2.

This study suggests a new approach to estimating frontal surface area distributions by generating geometrical tree models. The outcomes of the models come relatively close to reality but need refinement and calibration by performing additional measurements.

7 Recommendations

The constructed tree models give an indication of what is possible in terms of geometrical tree modelling for mangroves. In the end, we get a feeling of the relative importance of the various tree parts in terms of wave/current attenuation. Obviously, improvements can be made to obtain an even more reliable digital model that is able to approach the tree geometry as occurring in nature. To this end, we elaborate on two parts of the tree model: root (pneumatophores) model and canopy model. We will suggest improvements for both models. Additionally, we will make some general remarks that could pave the way for discussion. We start of with some recommendations regarding the root model.

7.1. Root model

The root models are constructed based on measurements on twenty-five roots for each tree type in combination with the amount of counted roots. We looked at four trees which is a relatively low amount of tree observations. More root measurements will positively contribute to the model certainty. Moreover, some additional measurements can be performed to (significantly) improve the quality of the model, namely:

- measure the root areas of trees as function of age (and neglect box dimensions)
- examine the effect of underground roots that radiate away from the main steam and determine how these affect the locations of aerial roots (pneumatophores)
- investigate what the relation is between above-ground biomass and root quantity. We suspect that these two are strongly linked, but a quantitative analysis would be beneficial to obtain accurate tree models in the end with the right root-canopy balance for *Avicennia m. vegetation*

7.2. Canopy model

We have seen that canopy geometries are complex structures that contains a large amount of information. For this study, four trees were measured and observed in detail to construct a model in the end. Obviously, measuring four trees is not a trustworthy representation of reality and more tree measurements give generally more model certainty as more data is used to calibrate the model. Some recommendations can be given for further measurement campaigns to improve *Avicennia m.* tree models:

- When applying Järvelä's tree-ordering scheme, it might be more convenient to measure the mean diameter of the largest order order tree stem instead of the diameter breast height (DBH). One could also establish a relation between both values as function of age since former articles mainly consider DBH.

- Tree growth stage/-age determines the collection and variety of branch orders that are present within its canopy system. It would be interesting to record at which age/growth stage transitions occur where additional branch orders will be added to the branch system.
- Perform additional measurements regarding: average diameters and standard deviations of branch orders for a large variety of tree types (age, density and multi-stemmed/single-stem). Also, additional branch length measurements can increase model certainty. Mainly, detailed measurements of large trees are missing at this point. These measurements will certainly improve the existing tree model. Besides, measurements of large *Avicennia m.* trees give an idea of what the limiting dimensions area for this tree species.
- Investigate the effect of flexible vegetation under wave attack. One should find out how much the vegetation deforms as function of the applied force. This will in turn affect the projected frontal surface area and thus wave dissipation through drag-type forces.
- A clear diameter decaying trend for branches has not been found during the course of this research study. However, more branch diameter measurements at fixed intervals could give a better picture of this naturally occurring phenomenon. Applying this information correctly in the tree model will yield an even more realistic tree model.

The above-mentioned factors can all improve the quality of the tree models. Diameter ratios between subsequent branch orders showed large variability in this research. More tree measurements will either confirm or contradict this. It might be more useful for mangrove tree modelling to come up with fixed ratios that represent a large data set of tree measurements. Alternatively, one could round off average values to more practical values of 1.5 or 2.0 and quantify the effect of these simplifications in terms of tree model accuracy. At last, one should investigate the differences between vegetation growing in nature and vegetation that grows in an artificial environment, such as a greenhouse.

7.3. General tree modeling recommendations

Every tree specimen has its own characteristics that will ultimately define its characteristic geometrical shape. It is advised to first observe the general tree structure before starting with measurements. One should look at the general branching structure, angles, amount of branch orders. Thereafter, one could measure the diameters and lengths of various branch orders, starting with the stem (which is most important). The relations that each (main)branch holds with its side branches are most important in modelling tree structure. These relations must be stored in an organized matter. Later on, one can apply these relations to construct subsequent branches. This is an iterative process and the best way to do this is by writing an algorithm in a coding environment.

Another recommendation is to observe the general root structure of a tree and see how this varies as function of tree characteristics such as age or size/biomass. This is key for obtaining a well balanced tree model that corresponds to reality.

References

Alongi, D. (2009). *The energetics of mangrove forests*. Springer.

Clarke, P. (1995). The population dynamics of the mangrove avicennia marina; demographicsynthesis and predictive modelling. *Hydrobiologia*, (295), 83–88.

Comley, B., & McGuinness, K. (2005). Above- and below-ground biomass, and allometry, of four common northern australian mangroves. *Australian Journal of Botany*.

Dalrymple, R., Kirby, J., & Hwang, P. (1984). Wave diffraction due to areas of energy dissipation. *Journal of Waterway, Port, Coastal & Ocean Engineering*, *110*(1).

Du, S., Lindenbergh, R., Ledoux, H., Stoter, J., & Nan, L. (2019). Adtree: Accurate, detailed, and automatic modelling of laser-scanned trees. *Remote sensing*, (11).

Duke, N., Kathiresan, K., Salmo III, S., Fernando, E., Peras, J., Sukardjo, S., Miyagi, T., Ellison, J., Koedam, N., Wang, Y., Primavera, J., Jin Eong, O., Wan-Hong Yong, J., & Ngoc Nam, V. (2010). Avicennia marina. the iucn red list of threatened species 2010: E.t178828a7619457.

Fu, W., & Wu, Y. (2011). Estimation of aboveground biomass of different mangrove trees based on canopy diameter and tree height. *Procedia Environmental Sciences*, (10), 2189–2194.

Giri, C., Ochieng, E., Tieszen, L. L., Zhu, Z., Singh, A., Loveland, T., Masek, J., & Duke, N. (2011). Status and distribution of mangrove forests of the world using earth observation satellite data. *Global Ecology and Biogeography*, *20*(1), 154–159.

Hackenberg, J., Morhart, C., Sheppard, J., Spiecker, H., & Disney, M. (2014). Highly accurate tree models derived from terrestrial laser scan data: A method description. *Procedia Environmental Sciences*, (5), 1069–1105.

Horstman, E., Dohmen-Janssen, C., Narra, P., van den Berg, N., Siemerink, M., & Hulscher, S. (2014). Wave attenuation in mangroves: A quantitative approach to field observations. *Coastal Engineering*.

Intarat, K., & Vaiphasa, C. (2020). Modeling mangrove above-ground biomass using terrestrial laser scanning techniques: A case study of the avicennia marina species in the bang pu district, thailand. *International Journal of Geoinformatics*.

Järvelä, J. (2004). Determination of flow resistance cause by non-submerged woody vegetation. *International Journal of River Basin Management*, *2*(1), 61–70.

Jordan, P., & Frohle, P. (2022). Bridging the gap between coastal engineering and nature conservation? *Journal of Coastal Conservation*, (26).

Jusoh, M., Aziz, N., & Inayatulla, O. (2016). Computational fluid dynamic simulation of flow velocities dissipation by mangroves roots structure. *ARPN Journal of Engineering and Applied Sciences*, *11*(6).

Kalloe, S., Hofland, B., Antolinez, J., & van Wesenbeeck, B. (2022). Quantifying frontal-surface area of woody vegetation a crucial parameter for wave attenuation. *Frontiers in Marine Science*, *9*.

Komiyama, A., Eong Ong, J., & Poungparn, S. (2008). Allometry, biomass, and productivity of mangrove forests: A review. *Aquatic Botany*, (89), 128–137.

Liénard, J., Lynn, K., Strigul, N., Norris, B., Gatziolis, D., Mullarney, J., Bryan, K., & Henderson, S. (2016). Efficient three-dimensional reconstruction of aquatic vegetation geometry: Estimating morphological parameters influencing hydrodynamic drag. *Estuarine, Coastal and Shelf Science*, (178).

Lovelock, C., Cahoon, D., Friess, D., Gutenspergen, G., Krauss, K., Reef, R., Rogers, K., Saunders, M., Sidik, F., Swales, A., Saintilan, N., Thuyen, L., & Triet, T. (2015). The vulnerability of indo-pacific mangrove forests to sea-level rise. *Nature*, *526*.

Maza, M., Lara, J., & Losada, I. (2021). Predicting the evolution of coastal protection service with mangrove forest age. *Coastal Engineering*, (168).

Maza, M., Adler, K., Ramos, D., Garcia, A. M., & Nepf, H. (2017). Velocity and drag evolution from the leading edge of a model mangrove forest. *Journal of Geophysical Research: Oceans*.

Maza, M., Lara, J. L., & Losada, I. J. (2021). Predicting the evolution of coastal protection service with mangrove forest age. *Coastal Engineering*.

Mazda, Y., Magi, M., Ikeda, Y., Kurokawa, T., & Asano, T. (2006). Wave reduction in a mangrove forest dominated by sonneratia sp. *Wetlands Ecology and Managament*.

Mazda, Y., & Wolanski, E. (2009). Hydrodynamics and modeling of water flow in mangrove areas.

Mazda, Y., Wolanski, E., King, B., Sase, A., Ohtsuka, D., & Magi, M. (1997). Drag force due to vegetation in mangrove swamps. *Mangroves and Salt Marshes*.

McIvor, A., Moller, I., Spencer, T., & Spalding, M. (2012). *Reduction of wind and swell waves by mangroves*. The Nature Conservancy; Wetlands International.

McMahon, T., & Kronauer, R. (1976). Tree structures: Deducing the principle of mechanical design. *Theor. Biol.*, *59*(1), 443–466.

Polidoro, B., Carpenter, K., Collins, L., Duke, N., Ellison, A., J.C., E., et al. (2010). The loss of species: Mangrove extinction risk and geographic areas of global concern. *Plos ONE*, *5*(4).

Prusinkiewicz, P., & Lindenmayer, A. (1996). *The algorithmic beauty of plants*. Springer-Verlag.

Purwiyanto, A., & Agustriani, F. (2017). Estimasi stok karbon mangrove (aboveground) di tanjung api-api, sumatera selatan. *Jurnal Ilmu dan Teknologi Kelautan Tropis*, *9*(2), 761–770.

Schiereck, G. (2012). *Introduction to bed, bank and shore protection*. VSSD.

Shlyakhter, I., Rozenoer, M., Teller, S., & Dorsey, J. (2001). Reconstructing 3d tree models from instrumented photographs. *IEEE engineering in medicine and biology magazine*.

Spalding, M., Kainuma, M., & Collins, J. (2010). *World atlas of mangroves (version 3.1)*. London (UK): Earthscan, London.

Suzuki, T. (2011). *Wave dissipation over vegetation fields* [Ph.D. thesis, Delft University of Technology].

Temmerman, S., Meire, P., Bouma, T. J., Herman, P. M., Ysebaert, T., & De Vriend, H. J. (2013). Ecosystem-based coastal defence in the face of global change. *Nature*.

Thampanya, U. (2006). *Mangroves and sediments dynamics along the coasts of southern thailand*. Taylor; Francis Publishers.

van Santen, P., Augustinus, P., Janssen-Stelder, B., Quartel, S., & Tri, N. (2007). Sedimentation in an estuarine mangrove system. *Journal of Asian Earth Sciences*, *29*, 566–575.

van Wesenbeeck, B., Wolter, G., Antolinez, J., Kalloe, S., Hofland, B., de Boer, W., Cete, C., & Bouma, T. (2022). Wave attenuation through forests under extreme conditions. *International Journal of River Basin Management*, *12*(1884).

Yang, J., Gao, J., Cheung, A., Liu, B., Schwendenmann, L., & Costello, M. (2013). Vegetation and sedimentation characteristics in an expanding mangrove forest in new zealand. *Estuarine, Coastal and Shelf Science*, *134*, 11–18.

A
Avicennia marina: background information

Figure A.1: Global distribution map of *Avicennia marina* vegetation

Observation	DBH (cm)	Height (m)	Observation	DBH (cm)	Height (m)
AM01	18.81	10.70	AM16	19.19	10.99
AM02	26.57	10.50	AM17	26.50	11.23
AM03	20.24	11.41	AM18	23.78	11.04
AM04	14.03	11.55	AM19	23.91	10.65
AM05	20.62	13.52	AM20	16.40	9.91
AM06	14.80	7.73	AM21	20.04	10.84
AM07	19.86	11.31	AM22	26.75	10.33
AM08	11.90	6.13	AM23	16.55	10.33
AM09	13.30	7.14	AM24	17.69	11.84
AM10	12.42	6.88	AM25	16.04	10.19
AM11	24.67	10.74	AM26	15.91	10.75
AM12	25.31	10.66	AM27	26.17	11.05
AM13	15.97	10.33	AM28	22.12	10.55
AM14	24.11	10.10	AM29	21.70	10.73
AM15	20.96	10.55	AM30	16.03	10.43

Figure A.2: Measured DBH values and heights of thirty sample trees of the type *Avicennia marina* in Bang Pu, Thailand (Intarat & Vaiphasa, 2020)

B

Root measurements

Open sapling [box 31]							Dense sapling [box 32]						
no.	H [cm]	D_{0h} [mm]	$D_{0.5h}$ [mm]	$D_{0.9h}$ [mm]	Dm/Db	Dt/Db	no.	H [cm]	D_{0h} [mm]	$D_{0.5h}$ [mm]	$D_{0.9h}$ [mm]	Dm/Db	Dt/Db
1	15,2	11,2	9,64	7,94	0,86	0,71	1	22,2	7,7	6,2	4,9	0,81	0,64
2	14,8	9,46	8,8	7,7	0,93	0,81	2	20,7	8,3	7	5,8	0,84	0,70
3	13,5	11,3	10	8,2	0,88	0,73	3	9,8	7,1	7	6,8	0,99	0,96
4	6,5	8	8	6	1,00	0,75	4	10,1	6,2	6,2	3,5	1,00	0,56
5	18,2	9,1	7,8	6	0,86	0,66	5	16,5	7	6	4,8	0,86	0,69
6	9,8	6,9	6,8	5	0,99	0,72	6	10,4	8,9	8,2	7,3	0,92	0,82
7	8,4	9	9	8,5	1,00	0,94	7	24	9	8	6,5	0,89	0,72
8	17,4	9	8,2	8	0,91	0,89	8	18,5	9,7	9,3	7,3	0,96	0,75
9	19	11,7	13	11	1,11	0,94	9	14,8	6,8	6,8	3,9	1,00	0,57
10	15,5	7,5	7,5	6	1,00	0,80	10	19	10	8,7	6	0,87	0,60
11	16	7	7	5,5	1,00	0,79	11	20,5	8	7,5	6	0,94	0,75
12	20,2	11,5	9	8	0,78	0,70	12	15,1	7	6,5	6	0,93	0,86
13	15,5	8,6	8	5,1	0,93	0,59	13	18,8	10,5	9,4	8	0,90	0,76
14	10,7	9,2	9,2	8,8	1,00	0,96	14	16,7	7	6,3	5	0,90	0,71
15	13,7	8,2	7,9	7,6	0,96	0,93	15	21,7	8	7	5,5	0,88	0,69
16	12	10,5	10	9,1	0,95	0,87	16	9,8	7,8	7,7	7,5	0,99	0,96
17	14,5	10,1	10	8	0,99	0,79	17	17,2	8,3	8	8	0,96	0,96
18	10,5	9,5	8,9	8	0,94	0,84	18	15,9	7,5	6	5,2	0,80	0,69
19	11,4	10,8	10	9,2	0,93	0,85	19	15,3	7,1	6	5	0,85	0,70
20	13,5	9,8	8	6,9	0,82	0,70	20	19	8,6	7,1	5	0,83	0,58
21	12,6	12	11,1	9,5	0,93	0,79	21	11,5	6	6	3	1,00	0,50
22	14	10,5	9,9	8,5	0,94	0,81	22	20,5	9	7	6,2	0,78	0,69
23	11,3	8	8	7	1,00	0,88	23	17	9,5	8	6,5	0,84	0,68
24	10,3	10	8,5	4,5	0,85	0,45	24	9,5	5	5	5	1,00	1,00
25	19,5	9,8	10,9	8,8	1,11	0,90	25	15,1	7	6,7	6	0,96	0,86

Figure B.1: Pneumatophore structure measurements for saplings

Open tree [box 12]							Dense tree [box 5]						
no.	H [cm]	D_{0h} [mm]	$D_{0.5h}$ [mm]	$D_{0.9h}$ [mm]	Dm/Db	Dt/Db	no.	H [cm]	D_{0h} [mm]	$D_{0.5h}$ [mm]	$D_{0.9h}$ [mm]	Dm/Db	Dt/Db
1	21	10,5	9	6,8	0,86	0,65	1	24	18,5	13,5	9,5	0,73	0,51
2	23,5	11	9	7,4	0,82	0,67	2	23,5	9	6	2,8	0,67	0,31
3	20	9	8	6	0,89	0,67	3	11,2	9	8	7	0,89	0,78
4	15	8	6,5	6	0,81	0,75	4	25,5	11	8,9	5,5	0,81	0,50
5	19	9	9	6	1,00	0,67	5	24,5	11,5	9	6,6	0,78	0,57
6	16,4	8,5	6,5	5,5	0,76	0,65	6	17,5	13	11	7	0,85	0,54
7	17	9,2	8,2	6,3	0,89	0,68	7	20,7	9	6,5	4,1	0,72	0,46
8	27	10,3	8	6,1	0,78	0,59	8	17,8	12,7	9,3	7,1	0,73	0,56
9	18	11,5	9	8	0,78	0,70	9	10	7	6	4	0,86	0,57
10	16,2	10	6,9	5,8	0,69	0,58	10	17,5	9,8	9,2	6,1	0,94	0,62
11	12,5	8	6	5	0,75	0,63	11	14	7	6,7	5,4	0,96	0,77
12	20	10,5	9,2	8,2	0,88	0,78	12	12	8,8	7,2	4,2	0,82	0,48
13	21,7	11	10,5	7,3	0,95	0,66	13	16	11,3	10	7	0,88	0,62
14	12,8	7,6	6,2	5	0,82	0,66	14	13,5	8,7	8	5	0,92	0,57
15	20	10	9,1	7,3	0,91	0,73	15	13	10	6,5	5,5	0,65	0,55
16	19	11,6	10	8	0,86	0,69	16	12	9,9	8,8	8	0,89	0,81
17	11	9	8	7,2	0,89	0,80	17	18,5	11,2	10	7,5	0,89	0,67
18	18,5	9,7	8,4	7	0,87	0,72	18	26	10,5	8,2	4,3	0,78	0,41
19	17	11	8	6,5	0,73	0,59	19	10	8,9	6,5	5,4	0,73	0,61
20	19,2	9,5	9	7	0,95	0,74	20	18	13	10,2	7,5	0,78	0,58
21	17	9,5	8,5	6,4	0,89	0,67	21	20	11,8	9,5	7	0,81	0,59
22	14	7,9	6,1	5,1	0,77	0,65	22	17,1	10,4	10,1	6,9	0,97	0,66
23	30	11	9,5	6	0,86	0,55	23	17,5	9	7,9	6	0,88	0,67
24	12	3,2	3	2,5	0,94	0,78	24	10,6	7,7	6,2	5,1	0,81	0,66
25	16	10	8,2	6	0,82	0,60	25	19,8	11,9	11	6,1	0,92	0,51

Figure B.2: Pneumatophore structure measurements for mature trees

C
Canopy measurements

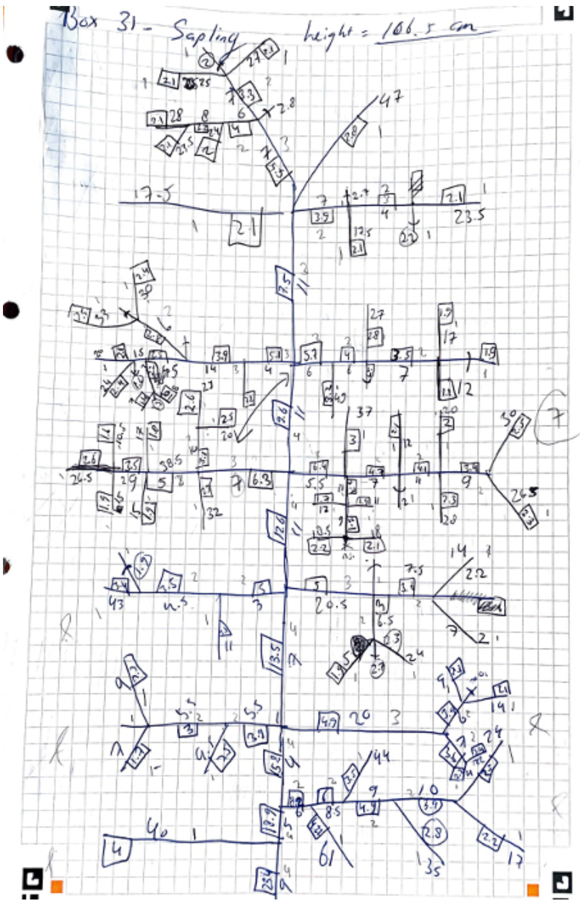

Figure C.1: Schematic drawing with measurements, box 31 (open sapling)

Figure C.2: Schematic drawing with measurements, box 32 (dense sapling)

D

Data storage & analysis - Python scripts

```python
# Tree structure data storage of the Greenhouse measurements from Deltares
# Specie: AVICENNIA MARINA
class treenode:
     #Every branch (node) is assigned attributes: branch order, diameter, length,
     #sidebranch start/base level w.r.t. main branch.
    def __init__(self, order, diameter, length, baseheight):
        self.order = order
        self.diameter = diameter
        self.length = length
        self.base_h = baseheight
        self.children = []
        self.parent = None

    #Function that forms links between branches: parent/child relationships
    def add_child(self, children):
        children.parent = self
        self.children.append(children)
```

Figure D.1: Class definition: creating an branch (object) with assigned properties

```python
#Tree(part) with highest order = 3:
if self.order == 3:
    d = self.diameter
    L3.append(self.length)
    if self.children:
        for i in self.children:
            if i.order == 2:
                A = []
                O32.append(i.diameter)
                L32.append(i.length)
                A.append(i.diameter)
                r3_2.append(d/np.mean(A))
                if i.children:
                    for j in i.children:
                        B = []
                        O21.append(j.diameter)
                        L21.append(j.length)
                        B.append(j.diameter)
                        r2_1.append(O32[-1]/np.mean(B))
            elif i.order == 1:
                C = []
                O31.append(i.diameter)
                L31.append(i.length)
                C.append(i.diameter)
                r3_1.append(d/np.mean(C))
```

Figure D.2: Part of the non-binary search tree algorithm, used for the analysis of data